Development of Active Trailer Steering Systems for Pickup Truck-Trailer Combinations

By
Priya Shastry

A thesis submitted to the
School of Graduate and Postdoctoral Studies in partial
fulfillment of the requirements for the degree of

Master of Applied Science in Automotive Engineering

Faculty of Engineering and Applied Science
University of Ontario Institute of technology
Oshawa, Ontario, Canada

August 2019

THESIS EXAMINATION INFORMATION

Submitted by: **Priya Shastry**

Master of Applied Science in **Automotive Engineering**

Thesis title: Development of Active Trailer Steering Systems for Pickup Truck-Trailer Combinations

An oral defense of this thesis took place on August 15th, 2019 in front of the following examining committee:

Examining Committee:

Chair of Examining Committee	Dr. Dipal Patel
Research Supervisor	Dr. Moustafa El-Gindy
Research Co-Supervisor	Dr. Jing Ren
Examining Committee Member	Dr. Xianke Lin
Thesis Examiner	Dr. Yuping He

The above committee determined that the thesis is acceptable in form and content and that a satisfactory knowledge of the field covered by the thesis was demonstrated by the candidate during an oral examination. A signed copy of the Certificate of Approval is available from the School of Graduate and Postdoctoral Studies.

ABSTRACT

Lateral dynamics of articulated vehicles continue to remain a subject of concern in the design of safety systems. Vehicle-trailer combinations tend to exhibit low lateral stability and poor maneuverability, especially under high-speed maneuvers, which lead to unstable motion modes such as jackknifing, trailer sway and rollover. Active safety systems such as Active Trailer Steering (ATS) have been widely studied to address these issues and ensure the safety of combination vehicles. Linear Quadratic Regulator (LQR) is a popular control technique to design ATS systems. Although this technique has demonstrated consistent results, this controller is not effective in the presence of parametric uncertainties. Therefore, a robust control strategy is proposed to improve the overall dynamic performance of the system. This research focuses on designing an ATS system for pickup truck and tandem-axle trailer combinations using the LQR and robust H-infinity (H_∞) control techniques. Numerical simulations are carried out using TruckSim and MATLAB/Simulink software packages, and the results are analyzed under high-speed performance measures.

Keywords: Articulated vehicles, active trailer steering systems, LQR, robust control, H-infinity, lateral stability, rearward amplification, offtracking, load transfer ratio

AUTHORS DECLARATION

I hereby declare that this thesis consists of original work of which I have authored. This is a true copy of the thesis, including any required final revisions, as accepted by my examiners.

I authorize the University of Ontario Institute of Technology to lend this thesis to other institutions or individuals for the purpose of scholarly research. I further authorize University of Ontario Institute of Technology to reproduce this thesis by photocopying or by other means, in total or in part, at the request of other institutions or individuals for the purpose of scholarly research. I understand that my thesis will be made electronically available to the public.

_____

Priya Shastry

Statement of Contributions

I hereby certify that I am the sole author of this thesis and that no part of this thesis has been published or submitted for publication. I have used standard referencing practices to acknowledge ideas, research techniques, or other materials that belong to others. Furthermore, I hereby certify that I am the sole source of the creative works and/or inventive knowledge described in this thesis.

ACKNOWLEDGEMENTS

† "When you go through deep waters, I will be with you." †

Isaiah 43:2

I would like to thank my supervisors Dr. Moustafa El-Gindy, Dr. Jing Ren and Dr. Xianke Lin for their support and valuable feedback. I would also like to thank BC Ministry of Transportation and Infrastructure for their contribution towards this research work and providing a foundation for this study.

I would like to thank my parents and brother -Nagesh, Leena and Pritesh Shastry- for their constant prayers, love and motivation throughout this journey. I am also particularly grateful to Aunty Randa who looked after me like her own during the most critical stages of this journey.

I would like to extend my gratitude to the members of the Multi-disciplinary Vehicle System Design Laboratory who have directly or indirectly contributed towards this research. A special mention of appreciation goes out to Smitha Vempaty whose guidance in the area of Active Trailer Steering was instrumental through each stage of this process.

I am profoundly grateful to Mutaz Keldani, who was my companion through the highs and lows of this journey. Words will never be enough to express the gratitude I have for the friend and strength that he has been. I would also like to extend my gratitude to Tushita, Saurabh, Hammad and Zeinab for their help and support throughout the stages of this work.

Last but definitely not least, a special thank you to all my friends - Ruhi, Asmy, Reshma, Shreya, Pooja, Joel, Surya, Gaurav, Presha, Kripa, Divya, Nidhi, Jovita, Ramesh, Abhilash and Prasanth for their patience, love and prayers.

Contents

List of Figures

List of Tables

Abbreviations

DOF	Degree of Freedom
RWA	Rearward Amplification
LTR	Load Transfer Ratio
CG	Center of Gravity
GVWR	Gross Vehicle Weight Rating
SLC	Single Lane Change Maneuver
DLC	Double Lane Change Maneuver
ATS	Active Trailer Steering
ATB	Active Trailer Braking
ARC	Active Roll Control
LQR	Linear Quadratic Regulator
PID	Proportional Integral Derivative
SMC	Sliding Mode Control
MRAC	Model Reference Adaptive Control
VGA	Variable Geometry Approach
LMI	Linear Matrix Inequality
FLC	Fuzzy Logic Control
DHIL	Driver-Hardware-In-the-Loop
MIMO	Multiple Inputs and Multiple Outputs

GA	Genetic Algorithm
ESC	Electronic Stability Control
NHTSA	National Highway Traffic Safety Administration
FMVSS	Federal Motor Vehicle Safety Standards
HIL	Hardware-In-the-Loop
RT	Real-Time
CFD	Computational Fluid Dynamics

Chapter 1

Introduction

1.1 Vehicle-Trailer Combinations

A vehicle-trailer system is composed of a towing/leading unit and a trailing unit, connected by a hitch at the point of articulation. These systems are commonly referred to as combination vehicles or articulated vehicles. In North America, due to the relevance of road transportation, these vehicles have gained immense popularity over the years for their applications in freight transfer [2]. Articulated systems can transport more goods, which in turn reduces transportation costs due to the requirement of fewer drivers per unit of cargo transported [3]. Moreover, the vehicle-trailer combinations are versatile and can be readily connected and disconnected, making it feasible for use. [4, 5].

The vehicle-trailer system is broadly classified as light vehicle (passenger cars or pickup trucks)-trailer combinations and heavy vehicle (tractor unit or semi-trailers)-trailer combinations [6]. The focus of this research, however, is on a vehicle-trailer combination composed of a light-duty pickup-truck and a tandem-axle gooseneck trailer.

In the United States, commercial trucks are classified on the basis of the vehicle's Gross Vehicle Weight Rating (GVWR). Classes 1-2 represent the light-duty trucks and have a GVWR limit of 4,536 kg. Classes 3-6 are the medium-duty trucks with a GVWR limit of 11,793 kg. Lastly, classes 7-8 are categorized as heavy-duty trucks with a GVWR of above 14,969 kg [7].

Gooseneck trailers are compatible with pickup trucks exclusively, and most of them can be classified as commercial trailers, owing to their heavy weight. This trailer is connected to a hitch mounted on the bed of the pickup truck, right above the rear axle. Some of the common uses of this trailer include transporting livestock, boats and are even used as car haulers and utility trailers [8].

1.2 Motivation

Although the benefits of vehicle-trailer systems are many, towing a trailer is generally accompanied by a number of unique challenges to motorists. Reports suggest that about 20% of the reported collisions involve rear-end collisions of vehicle-trailer combinations where the driver was at fault, and about 30% of the drivers claimed to have lost control of their vehicle [9].

Stability and dynamic performance have been a major concern for vehicle-trailer combinations. Due to the complexity in their configurations, these systems tend to exhibit undesired responses under varying payload properties, at high speeds and other external perturbations such as uneven roads and driver steering inputs [6]. This aspect can be challenging to drivers of light vehicles,

who sporadically tow recreational trailers and may not have an adequate understanding of the complexities in the dynamic behaviour of combination vehicles. Once the vehicle becomes unstable, gaining control over the vehicle-trailer combination is a difficult task [10]. This, in turn, can compromise the safety of the driver and other motorists and passengers. Therefore, the lateral stability of articulated vehicles is a topic of significance for researchers in the field of vehicle dynamics.

Vehicle-trailer combinations are vulnerable to unique unstable motion modes such as trailer sway, jackknifing and rollover. Trailer sway is a form of instability in which the trailer oscillates and in severe cases, leads to loss of vehicle control [6]. In severe cases, trailer sway may result in a phenomenon known as jackknifing. Jackknifing occurs when the articulation angle between the vehicle and trailer exceed a critical limit, due to which the driver loses control of the vehicle. Figures 1.1 and 1.2 depict trailer sway and jackknife scenarios experienced by articulated vehicles, respectively.

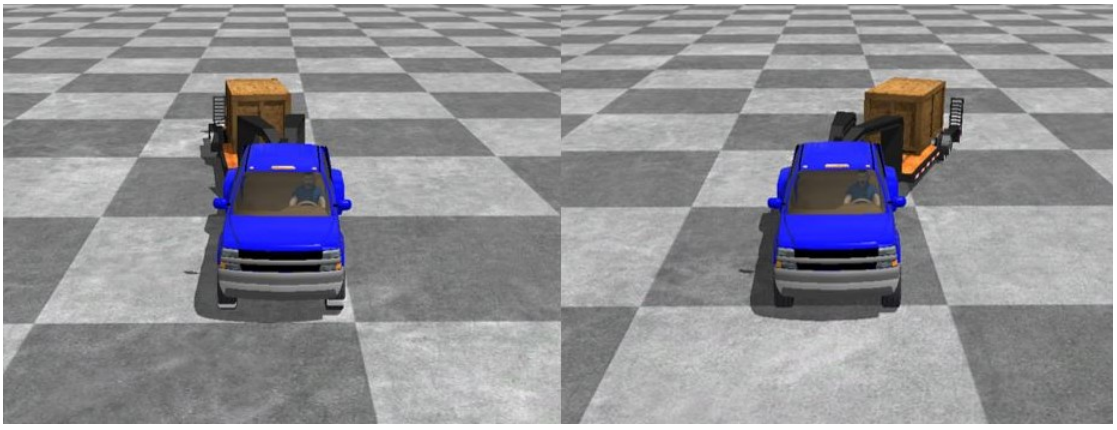

FIGURE 1.1: Trailer sway scenario

FIGURE 1.2: Pickup truck-trailer combination jackknife scenario

Finally, one of the most dangerous occurrences experienced by combination vehicles is the phenomenon of rollover. National Highway Traffic Safety Administration (NHTSA) defines rollover as any vehicle rotation of 90 degrees or more about any true longitudinal or lateral axis [11]. According to the data presented by NHTSA in 2005, 34.5% of the rollover rates that resulted in fatal crashes were experienced by utility vehicles, which is the highest in comparison to other vehicle types [11]. Rollovers occur as a result of high-frequency steering inputs, high-speed curved path negotiations, high-speed lane change maneuvers and load transfer [4, 12]. Figure 1.3 illustrates a rollover scenario experienced by vehicle combinations. The mentioned instabilities mostly occur at high speeds and have lead to fatal accidents, causing significant damages to life and property [4, 11].

FIGURE 1.3: Pickup truck-trailer combination rollover scenario

Therefore, in order to address the instability issues of light vehicle-trailer combinations, numerous active safety systems such as Active Trailer Steering (ATS) systems have been introduced [12–15]. Control strategies such as Linear Quadratic Regulator (LQR) have been extensively used for the design of active safety systems [4, 16, 17]. Due to its simplicity and superior performance, these controllers are the preferred controllers. However, LQR controllers are designed based on pre-defined system parameters. Therefore, these controllers fail to exhibit robustness in the presence of external disturbances, un-modelled dynamics and parametric uncertainties [16, 18]. Hence, in this study, a robust H_∞-based ATS system is proposed to address the robustness concerns and work effectively with the system's uncertainties.

1.3 Performance Measures

In this study, the main goal of the development of a controller is to ensure the robust and safe performance of a pickup truck-trailer combination at high speeds. In order to evaluate the effectiveness of the designed control system in terms of safety, a set of performance measures are applied to the combination vehicle. These safety-related performance measures were introduced by Ervin and Guy in 1986 [19] to examine the effect of various vehicle parameters on the dynamic performance under low and high speed maneuvers. Since the main focus of this study revolves around improving the lateral stability of a pickup truck-trailer combination at high speeds, the performance measures based on high-speed maneuvers are used to evaluate the authenticity of the controller. The high-speed maneuvers and their corresponding performance measures are described in detail below [19, 20]:

1. SLC maneuver
    (a) RWA ratio
    (b) LTR
    (c) Offtracking
2. Steady-state ramp-steer maneuver
    (a) Handling performance
    (b) Static Rollover Threshold (SRT)

1.3.1 Single Lane Change Maneuver (SLC) maneuver

1.3.1.1 Rearward Amplification (RWA) ratio

The RWA is defined as the ratio of the peak value of lateral acceleration at the mass Center of Gravity (CG) of the rearmost trailer to that of the leading unit during a lane change maneuver. This measure describes the tendency of trailers to over-respond or exhibit higher peaks of lateral acceleration values than the leading unit [20, 21]. It is considered as one of the most crucial measures used to evaluate an articulated vehicle's lateral stability at high speeds [22]. The SLC maneuver is emulated at a steering input of 0.4 Hz since it is at this input frequency that most articulated vehicles exhibit maximum RWA [23]. The RWA ratio is determined using the equation given below:

$$RWA = \frac{|\, A_{y2}(max)\,|}{|\, A_{y1}(max)\,|} \tag{1.1}$$

where, A_{y1} is the lateral acceleration of the pickup truck and A_{y2} is the lateral acceleration of the trailer. The peak lateral acceleration value of the trailer is generally larger than that of the leading unit, causing the RWA ratio to be greater than 1. Therefore, an RWA ratio of 1 is considered ideal since it indicates that the trailing unit follows the lateral dynamics of the leading unit [22].

1.3.1.2 Load Transfer Ratio (LTR)

LTR is the second performance measure used in this study to evaluate the effectiveness of the controller. LTR is defined as the absolute value of the difference between the total normal forces acting on the right and left sides of the articulated vehicle to the sum of the total normal forces [19]. LTR accounts for the

weight distribution across the left and right sides of the vehicle. The concentration of more weight on one side causes the vehicle to tilt or tip over, thus compromising the safety of the vehicle. LTR is represented by the equation given below:

$$LTR = \frac{|\, F_r - F_l \,|}{|\, F_r + F_l \,|} \tag{1.2}$$

where, F_r and F_l are the sum of the normal forces acting on the right and left sides of the pickup truck-trailer respectively. An LTR of 1 indicates complete lift-off of one of the sides of the vehicle [19].

1.3.1.3 Offtracking

The final performance measure under the rapid SLC maneuver is offtracking. Offtracking is defined as the lateral deviation between the path of the center of the pickup truck's first axle and the path of the center of the most severely offtracking axle of the last unit [19, 24, 25]. In this study, the improvement in offtracking of the vehicle with the ATS system is determined based on a comparison with the passive system, i.e. without the control system.

1.3.2 Steady-state ramp-steer maneuver

1.3.2.1 Handling performance

The steady-state handling performance pertains to the directional behaviour of the articulated vehicle during a turn under time-invariant conditions [26]. The handling characteristics of a vehicle is measured in terms of a gradient known as understeer coefficient and is represented as K_{us}. From the handling diagram,

K_{us} is the negative inverse of the slope of the handling curve at the required lateral acceleration. The steady-state handling characteristics are classified into three categories, namely, understeer, neutral steer and oversteer [26]. Understeer is defined as a phenomenon in which the slip angles at the front axles increase more sharply than the rear axle at increasing values of lateral acceleration. A vehicle is considered to be understeer if $K_{us} > 0$. Neutral steer is a phenomenon in which the slip angles at both the front and rear axles remain the same at increasing values of lateral acceleration. A vehicle is considered to be neutral steer if $K_{us} = 0$. Finally, oversteer is the phenomenon in which the slip angle at the rear axle increases more sharply than the slip angles at the front axles at increasing values of lateral acceleration. A vehicle is considered to be oversteer if $K_{us} < 0$ [26].

This measure is evaluated by constructing a handling diagram that depicts the relationship between the lateral acceleration of the vehicle and a parameter, $\frac{Lr}{U} - \frac{\delta}{N_g}$, where L is the wheelbase of the pickup truck, r is the yaw rate of the pickup truck, U is the constant forward speed, δ is the steering wheel angle and N_g is the steering gear ratio. This measure is also referred to as the "three-point measure" since the handling diagram of the vehicle is analyzed at three different points. The handling diagram represents the stability and control characteristics of a vehicle over a range of lateral accelerations [27].

First point: This point refers to the lateral acceleration at which the transition from understeer to oversteer takes place. The recommended value of transition from understeer to oversteer is 0.2 g. This ensures that the driver has reasonable steering control of the vehicle over a reasonable range of lateral acceleration before the onset of oversteer [27].

Second point: The understeer coefficient at this point is evaluated at a lateral acceleration of 0.3 g and based on standards [27], this coefficient should be higher than the critical understeer coefficient K_{cr}. The critical understeer coefficient is computed using $\frac{-La_g}{U^2}$. This ensures that the driver does not experience directional instability at critical speeds [28].

Third point: The understeer coefficient at this point is evaluated at a lateral acceleration of 0.1 g and based on standards, the coefficient should fall between $0-2$ deg/g. This ensures handling controllability of the vehicle within its normal operating range [28].

1.3.2.2 Static Rollover Threshold (SRT)

Static Rollover Threshold (SRT) is defined as the maximum level of lateral acceleration beyond which rollover of the vehicle occurs at steady-state [27]. The SRT value of the configuration is the lateral acceleration at which the inner wheel of the last axle lifts off the ground [19]. The recommended maximum SRT value is 0.4 g.

In this thesis, the performance measures are applied as follows:

1. Controller Evaluation
    (a) RWA ratio
    (b) LTR
    (c) Offtracking
2. Extreme case scenario
    (a) Handling performance

(b) Static Rollover Threshold (SRT)

(c) Rearward Amplification (RWA) ratio

(d) LTR

(e) Offtracking

1.4 Thesis Contributions

The contributions of this thesis are as follows:

- Derived a linear 3-DOF yaw-plane model of a pickup truck-trailer combination and validated its dynamics against a nonlinear TruckSim model. This model was further used to develop the controllers mentioned below.
- Designed and implemented an LQR-based ATS system to enhance the dynamic performance of the pickup truck-trailer combination at high-speeds.
- Developed a robust H_∞-based ATS system to improve the robustness of the pickup truck-trailer combination at high speeds and under the influence of varying system parameters.
- Evaluated the effectiveness of the LQR and H_∞ based ATS systems by comparing the dynamic performance of the controlled vehicle with that of the uncontrolled one, for 12 different operating cases.
- Utilized the safety-related performance measures such as RWA ratio, LTR and offtracking to gauge the improvement in safety and performance of the controlled articulated vehicle with respect to the uncontrolled one.

1.5 Thesis Organization

The rest of the thesis is structured as follows:

Chapter 2 provides a detailed literature survey on articulated vehicles and the active safety systems employed to these vehicles to improve their lateral stability and maneuverability. This chapter also delineates the various types of controllers used, with emphasis on LQR and H_∞ control techniques.

Chapter 3 introduces the linear vehicle model and its validation with the nonlinear TruckSim model. Finally, an eigenvalue stability analysis is conducted over a range of payload weights and trailer CG distances to examine the stability boundaries of the derived linear model.

Chapter 4 deals with the synthesis of the LQR and H_∞ controllers presented in this study. It also details the theory behind the mentioned control systems and describes the TruckSim-MATLAB/Simulink co-simulation environment for each controller.

Chapter 5 introduces an extreme case scenario of the vehicle configuration based on the pickup truck's maximum hauling conditions. The dynamic behaviour of the configuration is analyzed at high speeds and based on the results obtained, another extreme case configuration with improved dynamic characteristics is proposed.

Chapter 6 presents the performance of the developed LQR-based and H_∞-based ATS controllers. Based on the results obtained, a comparative study is carried out to investigate the safety aspect of the vehicle, by the application of established performance measures.

Chapter 7 concludes and presents recommendations for possible future work.

Chapter 2

Literature Review

2.1 Introduction

This chapter presents a general survey on the modelling and safety systems of combination vehicles. It also includes a comprehensive review on the ATS systems and methodologies previously adopted by researchers. Furthermore, the control techniques employed for the implementation of ATS systems are discussed in detail.

2.2 Stability of Articulated Vehicles

Combination vehicles tend to exhibit various undesirable responses, especially under loaded conditions and at high speeds. As two pivot-connected units, the trailer is susceptible to instabilities such as trailer sway, jackknife and rollover. Additionally, the handling performance of the vehicle towing the trailer is compromised due to the dynamic and kinematic influences from the trailer [6, 10,

29]. Studies have emphasized the influence of physical parameters of the vehicle and trailer through simulations and experimental testing. The effects of trailer parameters on the lateral stability of combination vehicles were demonstrated by Collins and Wong [30] in 1974. The authors suggested that parameters such as hitch loading, trailer lengths and weights adversely influenced the stability and handling of vehicle-trailer systems. Kurtz et al. [29] used analytical modelling, simulations and road testing to study the effect of system parameters on the stability of articulated vehicles. The authors confirmed that the trailer's CG location is a critical factor in the trailer's stability. In 2008, Darling et al.[31] carried out an extensive experimental study on car-trailer systems. A detailed sensitivity analysis suggested that variations in trailer characteristics such as yaw inertia, load distribution and trailer axle position have a significant influence on the high-speed stability of the system.

2.3 Vehicle Systems Modelling

Vehicle systems are complex and inherently nonlinear. The modelling of vehicle systems is the initial and most crucial part of designing a control system. In order to understand the dynamics of articulated vehicles, a number of linear and nonlinear mathematical models have been proposed by researchers.

In a study presented by Mokhiamar [32], a 15-DOF nonlinear model of an articulated vehicle was developed using MATLAB/Simulink. This model took into account nine motions of the vehicle units and six motions of the wheels. A nonlinear 29-DOF car-trailer model was employed by M. Plöchl et al. [33] to stabilize the unfavourable behaviour of vehicle-trailer combinations. Fratila

and Darling [34] developed a complex car-caravan model with 24-DOF in a simulation package known as Bath*fp*. The model was composed of nonlinear tire and suspension characteristics, in an attempt to accurately predict the handling and stability of the combination at high speeds.

Sustersic [35] also demonstrated vehicle-trailer instabilities and the system was modelled using ADAMS software. This study also incorporated the aerodynamic influences obtained from Computational Fluid Dynamics (CFD). Sharp and Fernandez [36] designed an elaborate 32-DOF mathematical model, using AutoSim - a dynamic analysis software.

Collins [30], Hac et al. [10] investigated the effects of parameter variations of various trailer configurations using a simple linear yaw-plane model of a car-trailer system. Anderson and Kurtz [37] studied the handling characteristics of car-trailer systems using 4-DOF and 6-DOF vehicle models. They showed that the results obtained with the simple 4-DOF model were as accurate as those obtained with the complex 6-DOF model.

Deng[38], Sun et al. [39], Ellis [40] and other researchers examined the lateral dynamics of vehicle-trailer combinations using a 3-DOF linear yaw-plane model, that neglects the effects of pitch and roll motions of these systems. These models were extensively used to design active safety systems to improve the lateral stability of a car-trailer system under various operating parameters. The versatility of the 3-DOF linear yaw-plane model was demonstrated by [41, 42] in their analysis and comparison of various active control schemes. The applicability of various car-trailer models for the design of active safety systems was investigated in-depth by He and Ren [43]. A linear 3-DOF, a nonlinear 4-DOF and a nonlinear 6-DOF were generated and compared with a CarSim car-trailer

model. The study confirmed that the linear 3-DOF vehicle model is suitable to predict the lateral stability and in good agreement with the nonlinear vehicle models under low lateral acceleration maneuvers.

The application of nonlinear mathematical models for the design of controllers has been recommended by many researchers [17, 39, 44] in the past, due to its reliability and high fidelity. However, the size and complexity of these models are known to decrease the computational efficiency of simulations. Due to its simplicity, linear mathematical models are generally preferred for the design of control systems, provided the necessary precautions are taken to ensure that important dynamic features are not lost [5, 43, 45].

2.4 Safety Systems for Articulated Vehicles

In order to enhance the safety of single-unit vehicles (cars, SUVs, minivans), the FMVSS (Federal Motor Vehicle Safety Standards) 126 vehicle standard was issued in North America, that mandates all vehicles from 2012 model year, to be equipped with electronic stability control (ESC) system [46]. An ESC system can generate a yaw moment that enhances the lateral stability of the vehicle without driver intervention, during evasive steering maneuvers. Research suggests that this system improves vehicle stability and path-following performance under emergency maneuvers [47].

However, ESC systems are only applicable to single-unit vehicles and do not take external units, such as trailers, into account. Combination vehicles are highly susceptible to unique unstable motion modes due to their multi-unit

configuration, which can lead to fatal accidents [5, 48]. Moreover, in comparison to a single-unit vehicle, the driver of the combination vehicle has to also deal with issues such as trailer oscillation, poor path-following and possible instabilities [6]. Therefore, to strike a balance between the handling performance of the towing vehicle and overall system stability, several passive and active safety systems have been proposed.

2.4.1 Passive Safety Systems

Majority of the vehicle-trailer systems, till date, employ passive mechanisms to solve issues related to tire scrubbing and maneuverability [14, 42].

Mechanisms such as the Hensley arrow and Equal-i-zer are commercially available to improve the lateral stability of articulated vehicles. The Hensley arrow uses a mechanical linkage system to restrict the lateral movement of trailers [49]. On the other hand, another system known as the Equal-i-zer is a 4-point sway control that employs a combination of rotational friction sway control and rigid trailer brackets [50].

Sorge [51] suggested the application of a four-bar linkage between the lead unit and the trailer in place of the conventional pintle hitch, to improve the stability and maneuverability of the system. Sharp and Fernandez [36] proposed the inclusion of a coulomb friction damper at the pintle pin to stabilize the swaying motion of combination vehicles.

However, the systems above improve the maneuverability and reduce lateral tire forces exclusively in low-speed, steady-state maneuvers. This occurs at the cost of poor high-speed performance. At high speeds and transient maneuvers, these systems cause higher lateral accelerations, poor handling and poor

tracking [13, 14, 52]. Additionally, crucial parameters such as tire cornering stiffness and weight distribution, that affect the lateral stability of articulated vehicles tend to vary under different operating conditions. Therefore, since the behaviour of these systems alters with varying parameters, the stability of combination vehicles cannot be guaranteed with the aforementioned passive systems. Such drawbacks of these systems have been well documented by a number of researchers in the past [10, 36, 41, 43].

2.4.2 Active Safety Systems

Several active control strategies have been proposed in order to address the safety issues associated with combination vehicles. Active control techniques such as Active Trailer Braking systems (ATB) [5, 10, 18, 39, 41, 48], Active Trailer Steering (ATS) systems [12–15], Active Roll Control (ARC) [53–55] and Variable Geometry Approach (VGA) [41, 42, 56] have been proposed to improve the handling, stability and maneuverability of articulated vehicles.

Rafay et al. [41] evaluated and compared the performance of three stability control techniques for car-trailer systems, namely, ATB, ATS and VGA. The results obtained from numerical simulations demonstrated that the performance of the combination vehicle was far more superior with these stability control systems. It was also concluded that ATS and ATB control strategies have great promise. In a similar study carried out by Smitha and He [42], the concept of adaptive control approach was introduced as a method to maintain the lateral stability of a car-trailer system, irrespective of the impact due to external factors such as road and climatic conditions.

2.4.2.1 Active Trailer Braking Systems (ATB)

One of the most commonly investigated and cost-effective active safety systems for vehicle-trailer combinations is the ATB system [4, 5, 18, 36, 48]. This strategy has been used extensively to improve the lateral stability and handling of articulated vehicles at both low and high speeds [4, 5]. The main idea behind the ATB control is the utilization of an active yaw moment generated from the differential braking system of the trailer to control the yaw motion of the trailer, thus stabilizing the vehicle system.

2.4.2.2 Active Trailer Steering Systems (ATS)

Although the many advantages of ATDB have been highlighted in the past, this system needs to slow down the vehicle to operate. For a steady intervention of the control system, the constant application of brakes is necessary, which can cause undesired speed reduction and excessive wear of brake-lining and tires. This aspect necessitates the need for a control system that can be used continuously during high-speed maneuvers, without aggressive interaction. Studies have also reported increased improvement in vehicle dynamics during low-speed maneuvers using ATS [25].

Hata et al. [57] implemented a control technique for an ATS system on medium-duty trucks that focused on improving the path following ability of the trailer at low speeds. A similar approach was proposed by Notsu et al.[58] on a tractor semi-trailer combination, called the *coupling point path follow control*. In this strategy, the rear end of the combination was manipulated to follow the path of the hitch point. This proposition, however, was not pursued further due to a number of drawbacks.

In an elaborate study carried out by Odhams et al. [59], a path-following steering control strategy was designed and physically tested on an experimental tractor semi-trailer at both low and high speeds. The fidelity of this controller was further established through TruckSim / MATLAB simulations, which were validated against experimental data. It was concluded that the active steering systems presented above reduced off-tracking, trailer sway and tire wear.

Cheng and Cebon [60] introduced a 'virtual driver' steering model for the design of an optimal ATS algorithm. This controller optimized a combination of lateral load transfer and path-tracking error to enhance the roll stability of a tractor semi-trailer, especially during transient maneuvers.

In order to address the problems associated with articulated vehicles at high speeds, Cheng et al. [14] derived high-speed path-following and roll stability controllers using ATS. The novelty of this research was the introduction of a strategy to switch between the two controllers when required. This approach resulted in improved path tracking and roll stability in both steady-state and transient maneuvers.

Rangavajhula and Tsao [61] designed an ATS technique for articulated vehicles that steered the front trailer axles proportionately to the articulation angles. The optimal control design used in this study minimized both off-tracking and RWA of the vehicle combination.

A benchmark investigation on two control algorithms for ATS systems of Articulated Heavy Vehicles (AHV) was carried out by Ding et al. [2]. Fuzzy Logic Control (FLC) and LQR techniques were applied and evaluated using co-simulation in TruckSim and Simulink environment. Two road test scenarios: a 90-degree intersection turn and an SLC maneuver, were used to compare

the directional performance of the ATS systems based on the two controls algorithms. Simulation results demonstrated superior stability and maneuverability of AHVs with the integrated control systems.

In 2013, Jujnovich and Cebon [13] developed an ATS controller that included aspects of low and high speed steering controllers. Feedback, feed-forward and *model matching* strategies were utilized to ensure that the rear of the trailer followed the path of the fifth-wheel at both low and high speeds. TruckSim simulations demonstrated improved maneuverability at low speeds and reduced off-tracking at high speeds. The controller was also able to reject external disturbances that affect the yaw and lateral dynamics of articulated vehicles. This study, however, did not account for low friction conditions.

2.5 Control Techniques for Active Trailer Steering Systems

Till date, several control strategies have been investigated for the implementation of ATS systems in articulated vehicles. Control systems such as Proportional Integral Derivative (PID) [13], LQR [2, 5, 22, 41], Fuzzy logic control [2, 62], H_∞ [15, 63, 64] and Sliding Mode Control (SMC) [65–67] have been explored for ATS systems in articulated vehicles.

2.5.1 Linear Quadratic Regulator (LQR) Control Technique

LQR control is one of the most commonly investigated control systems for active steering systems. This technique has been extensively applied in ATS systems to augment the lateral stability and maneuverability of articulated vehicles. LQR is used to formulate optimal control gains to attain an optimal trade-off between low-speed handling and high-speed lateral stability [68–70]. Furthermore, these controllers are relatively easier to synthesize and perform much better than PID [5, 12, 15, 71].

Palkovics and El-Gindy [16] presented an active steering control strategy to improve the handling characteristics of heavy vehicles. The LQR controller was designed to minimize the states of the vehicle combination. A similar strategy was also adopted by Hac et al. in 2008 [10] and El-Gindy et al. [21] in 2001. Rangavajhula and Tsao [61] implemented an LQR controller for the development of an ATS system for a tractor and three full trailers. The controller was designed to reduce off-tracking and simultaneously minimize the RWA ratio of the vehicle system under standard maneuvers. In a study carried out by Kim et al. [70], an LQR-based active steering controller was designed to follow the desired yaw rates of the reference tractor and trailer and also minimize the units' CG side-slip angles. The proposed control technique worked well on both gentle as well as sharp curves. Recently, Warrier [17] proposed an LQR-based ATS controller to reduce the swept path width and eliminate trailer swing of an articulated vehicle during cornering. Using a nonlinear vehicle model, the controller was designed to follow the desired yaw rates and simultaneously minimize the CG side-slip angles of the tractor and trailer. The effectiveness of

the control system was evaluated and validated with the aid of simulations under a turning maneuver. The obtained results elucidate significant swept path reduction of the tractor-trailer.

Although numerous studies have established the efficiency of LQR-based ATS controllers in the directional performance of articulated systems, these controllers exhibit robustness concerns. Most of these controllers are designed under constant operating conditions and parameters. However, in reality, a vehicle system is highly complex, and its parameters and external disturbances are constantly changing [5, 12, 15, 71]. Therefore, in order to control a complex vehicle system, it is crucial to adopt a robust control technique that can account for the varying system uncertainties.

2.5.2 Robust Control Techniques

Robustness to parameter uncertainties, external disturbances and modelling inaccuracies is a vital part of control system design. This is because, in real applications, the plant to be controlled is far more complex, nonlinear and vulnerable to external disturbances [1]. Systems that can function under the effect of external variations and uncertainty are deemed robust. It is imperative for every control engineer to take into account the vulnerability of real-world dynamic systems to perturbations such as external disturbances, nonlinearities, parametric uncertainties and many others [72]. A considerable amount of work has been done in order to address robustness concerns.

Gain Matrix linear Interpolation (GMI) is a method used to improve the robustness of the LQR controller [73]. Recently, in a study conducted by Keldani et al. [73], a gain-scheduling LQR-based ATS control algorithm was introduced

to augment the robustness of the conventional LQR-based controller. The effectiveness of the proposed controller was evaluated at various forward speeds using numerical simulations, under an SLC maneuver. Results depicted that the proposed robust ATS controller significantly improved the RWA ratio, directional performance and lateral stability of the car-trailer system. The Linear Matrix Inequality (LMI)-based LQR technique is also used to augment the robustness of complex systems. In a study by Zhituo Ni and He [74], the robust ATS controller for the A-train Double proposed was designed using an LMI-based LQR technique. The uncertainties considered in the design of this controller were: vehicle forward speed and time constant of the ATS actuator model. The results obtained using numerical and Hardware-In-the-Loop (HIL) Real-Time (RT) simulations were in good agreement. The robust ATS controller successfully enhanced the performance of the A-train Double at both low and high speeds and also improved the RWA ratios of the vehicle system.

A well established robust control strategy is μ-synthesis. This controller has been applied by several researchers in the past to acknowledge robustness issues of complex systems [5, 12, 75]. In a study conducted by Yin et al. [76], the robust μ-synthesis technique was applied in the design of an active steering system. The control performance was evaluated using a linear vehicle model with tire cornering stiffness as the uncertain parameter. The robustness of the controller and its feasibility was assessed experimentally using HIL. Sikder [12] suggested a μ-synthesis controller for ATS of a B-train Double to deal with system uncertainties such as measurement and system noises. The controller's behaviour was analyzed under a random combination of 13 parametric uncertainties that depict poor vehicle dynamics.

Sliding Mode Control (SMC) is another frequently used robust control technique. The main advantages of sliding mode include simple implementation design and insensitivity to parameter variations and external disturbances [77]. This control technique has been widely used to control complex, nonlinear articulated vehicles with uncertainties [65–67]. SMC works on the basis of a high-frequency control switching approach, which is robust and accurate. However, this high-frequency control switching is responsible for the dangerous chattering effect, which tends to damage mechanical actuators (steering, brakes) [12, 66, 78].

Model Reference Adaptive Control (MRAC) is another control technique that can guarantee both stability and performance over a range of varying parameters [79]. This method has been adopted by Smitha and He [42] and Wang [71] to actively steer trailer axles of articulated vehicles. The results in both cases were examined using numerical simulations, and Wang [71] justified the effectiveness of this controller using Driver-Hardware-In-the-Loop (DHIL)-RT simulation. This technique demonstrated superior lateral dynamics of articulated vehicles despite parametric uncertainties such as trailer payloads and vehicle forward speeds.

As mentioned earlier, robustness is a crucial criteria for the design of controllers, and its importance has been highlighted by numerous researchers in the past [2, 5, 12, 39, 69]. In reality, the system to be controlled is complex and nonlinear and comprise of Multiple Inputs and Multiple Outputs (MIMO). Although nonlinear control techniques, such as Sliding Mode Control (SMC), exist, they are difficult to tune for acceptable performance.

H_∞ control is a linear control technique that was introduced in 1980 and ever

since, it has been regarded as a powerful tool for stabilizing uncertain complex systems. This technique is not just robust to uncertainties, but it is also capable of guaranteeing system stability [1].

This control technique has been widely used in the field of vehicle control. A four-wheel steering (4WS) controller was designed using H_∞ control strategy to improve the transient handling stability of a 4WS vehicle at high speeds [80]. The control algorithm was designed based on yaw rate tracking and effectively reduced peak values of yaw rates, lateral accelerations and side-slip angles under high-speed maneuvers. A novel H_∞-based active front steering system integrated with electric power steering was introduced by Zhao et al. [81]. A satisfactory steering feel and robust steering and performance were selected as the control objectives of this controller. Simulation results validated the effectiveness of this controller. Sun and Yan [82] proposed a novel H_∞ fuzzy control design using the Lyapunov function. The feasibility of this control technique was evaluated on a computer-simulated truck-trailer system. Güvenç et al.[83] developed a robust 2-DOF steering control to improve the yaw dynamics of a passenger car. A Linear Parameter-Varying (LPV) H_∞ control was synthesized based on six operating scenarios of vehicle speed and road friction coefficient. The controller was designed to provide corrective steering action only when required. The effectiveness of this control algorithm was evaluated using linear and nonlinear simulations. In a similar study later in 2009, Güvenç et al. [84] evaluated the effectiveness of the robust controller using HIL-RT simulations. Horiuchi et al. [85] introduced an active steering control approach using 2-DOF H_∞ control strategy. This system was composed of a feed-forward controller to

ensure reasonable command tracking and a feedback controller to satisfy robustness requirements. The efficiency of this control system was demonstrated through simulations and ground tests on an experimental vehicle.

H_∞ control strategy for ATS systems in articulated vehicle systems is a subject that is steadily gaining recognition in the world of research. In a recent study carried out by Sadeghi et al. [64], a robust steering-based controller for an A-double combination vehicle, equipped with a steerable dolly, was developed. The controller synthesis was formulated as an H_∞-type design problem based on LMI optimization. The control objective was to ensure robust stability and performance of the vehicle under the influence of parametric uncertainties such as tire cornering stiffness and moment of inertia of the semi-trailers. The robustness of the controller was verified by conducting simulations on both linear and nonlinear models and significant improvement in the lateral dynamics of the A-double was observed. Hingwe et al.[86] suggested an LPV H_∞ control technique for the automated lane keeping of a tractor-trailer combination. By incorporating the LPV-based design, the authors were able to synthesize a velocity-dependent controller that demonstrated superior performance. Kapoor [15] recommended the application of mixed-sensitivity H_∞ control technique for the ATS system of a B-train Double. The robust controller was optimized for a speed range of 40 to 120 km/h by the application of Genetic Algorithm (GA). This control technique enhanced the performance of the vehicle system under both SLC and Double Lane Change (DLC) maneuvers. The controller also demonstrated excellent yaw reference tracking and path following.

2.6 Summary

This chapter reviewed the various safety systems for articulated vehicles, with special emphasis on ATS systems. Literature suggested that these systems can effectively improve the dynamic behaviour of articulated vehicles under various scenarios. Researchers reported significant improvement in offtracking, RWA and lateral load transfer on the application of ATS systems to articulated vehicles. Numerous control techniques such as PID, SMC and fuzzy logic have been used for the synthesis of ATS systems. The most popular technique is the LQR control technique. However, numerous studies indicated that this control technique fails to exhibit robustness in the presence of external disturbances and system uncertainties. For this reason, many researchers have proposed the use of robust control systems such as SMC, μ-synthesis and H_∞. H_∞ is a control system that can overcome the effects of operating uncertainties to achieve robustness of the system.

Chapter 3

Vehicle System Modelling and Stability Analysis

3.1 Introduction

In this chapter, a 3-DOF yaw-plane linear model is derived and validated against a nonlinear TruckSim model. It is imperative to ensure that the mathematical model used for the development of the ATS system is stable over a reasonable operating range. Therefore, the stability boundaries of the linear model are evaluated using the eigenvalue sensitivity analysis. This analysis is carried out under varying vehicle parameters, i.e. trailer's payload weights and CG distances.

3.2 3-DOF Yaw-Plane Linear Model

Vehicle system modelling is the most crucial and foremost part of controller design. In this study, a 3-DOF yaw-plane linear model is adopted for the design

of an ATS system. The model is developed by deriving the governing equations of motion of the combination vehicle, based on Newton-Euler's equations of motion. The vehicle system comprises of a pickup truck and a tandem-axle gooseneck trailer. The two vehicle units are connected by a hitch located on the rear axle of the pickup truck, as illustrated in Figure 3.1. The schematic representation of the pickup truck-trailer combination is given in Figure 3.2.

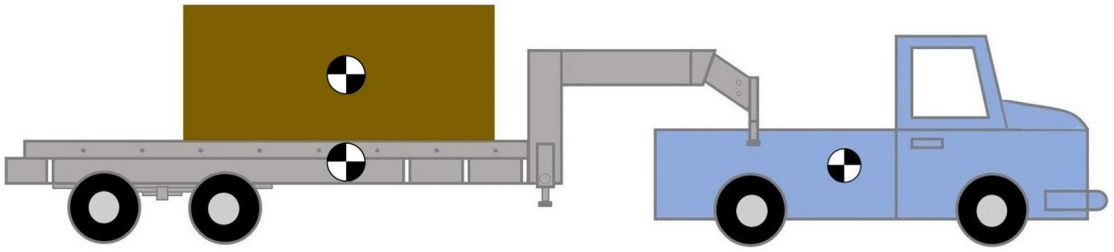

FIGURE 3.1: Pickup truck and gooseneck combination

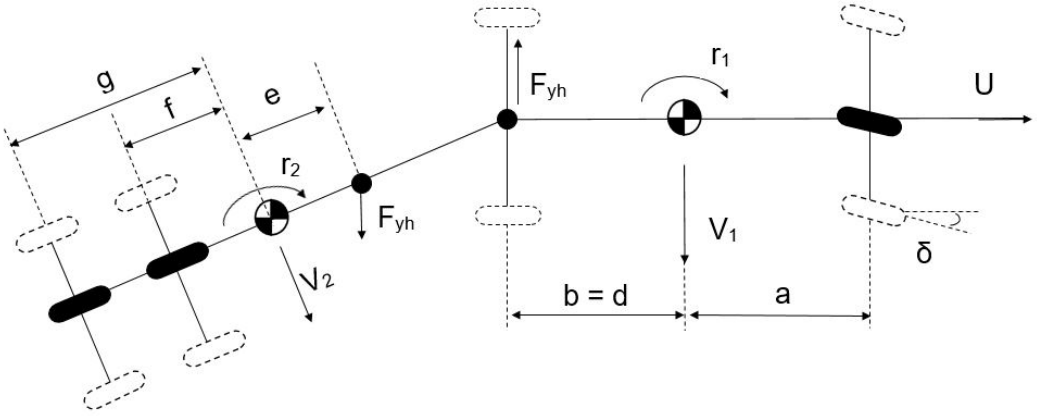

FIGURE 3.2: Schematic representation of the 3-DOF vehicle model

The 3-DOF model was developed using the body-fixed coordinate system with three independent motions, namely, lateral velocity of the pickup truck and yaw rates of the pickup truck and trailer. The assumptions considered for the modelling of the 3-DOF system are [5, 12, 15, 41, 73]:

1. The vehicle is moving at a constant forward speed U.

2. Small angle approximations are applicable for the articulation and steering

angles.

3. The pitch and roll motions are neglected.

4. The aerodynamics and braking forces are neglected.

5. Linear tire model is used.

The equations of motion of the pickup truck are:

$$m_1(\dot{V}_{y1} + Ur_1) = F_{y1} + F_{y2} - F_{yh} \tag{3.1}$$

$$I_{z1}\dot{r}_1 = aF_{y1} - bF_{y2} + dF_{yh} \tag{3.2}$$

The equations of motion of the trailer are:

$$m_2(\dot{V}_{y2} + Ur_2) = F_{y3} + F_{y4} + F_{yh} \tag{3.3}$$

$$I_{z2}\dot{r}_2 = -fF_{y3} - gF_{y4} + eF_{yh} \tag{3.4}$$

Based on hitch kinematics, the lateral motion of the articulation point is given by:

$$\dot{V}_{y1} - \dot{V}_{y2} - \dot{r}_1 d - \dot{r}_2 e = -Ur_1 + Ur_2 \tag{3.5}$$

The lateral tire forces are given by:

$$F_{yi} = -C_i \alpha_i, \tag{3.6}$$

where, i takes values between 1-4 representing the 4 axles of the vehicle combination, C_i and α_i is the cornering stiffness and slip angle of the tire respectively. The above governing equations of motion can be represented in state-space

form. The state-space equation of the 3-DOF pickup truck and trailer combination can be expressed as:

$$\dot{\mathrm{x}}(\mathrm{t}) = Ax(t) + Bu(t) \tag{3.7}$$

$$y(t) = Cx(t) + Du(t) \tag{3.8}$$

where, x(t) is the state variable vector and it is defined as $x = [\,V_{y1} \quad r_1 \quad V_{y2} \quad r_2]$. A is the state matrix, B is the input matrix and control input u is $[\delta_3 \quad \delta_4]^T$, where δ_3 and δ_4 represent the steering angles of the two trailer axles. C is the output matrix and D is the feedforward matrix. More details are offered in the Appendix.

3.3 Nonlinear TruckSim Model

The TruckSim software used in this study is an efficient method for simulating nonlinear multi-axle vehicle models. Its comprehensive user interface enables the user to analyze heavy vehicles under a variety of complex test scenarios. It is a useful analysis tool that is used by industry and researchers to analyze vehicle performance characteristics and design active safety systems. TruckSim models have been extensively validated against experimental data in the past [45, 87, 88].

The sprung masses of the pickup truck and trailer are regarded as rigid bodies with six Degrees of Freedom (DOF); three translating motions in the longitudinal, lateral, vertical directions and three rotating namely, roll, pitch and yaw angular motions. The gooseneck trailer's hitch is modelled as a joint about

which roll, pitch and yaw motions are permitted. The axles exhibit roll and vertical motions while the tires and suspensions have nonlinear characteristics [5]. Figure 3.3 depicts the pickup-truck configuration with a tandem-axle gooseneck trailer in TruckSim. Figure 3.4 depicts the TruckSim user interface.

FIGURE 3.3: Configuration of a pickup truck with a tandem-axle gooseneck trailer in TruckSim

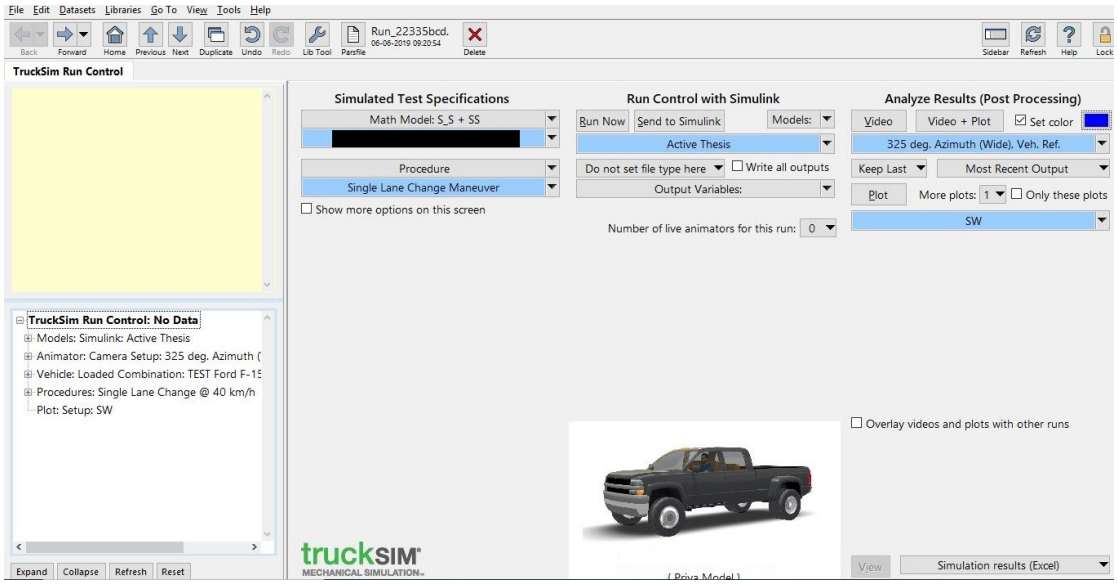

FIGURE 3.4: TruckSim user interface

3.4 Model Validation

To establish the accuracy of the linear 3-DOF model, it is validated with the nonlinear TruckSim model using an open-loop simulation technique. The dynamic responses of the 3-DOF model are compared with the responses of the nonlinear TruckSim model. In this study, both the models are subjected to an open-loop test under an SLC maneuver [4, 5]. The simulated steering input is a single-cycle sine wave fixed at a frequency of 0.4 Hz, and the forward speed is kept constant at 60 km/h [5]. The steering input is illustrated in Figure 3.5, and the block diagram of the open-loop environment for validation is depicted in Figure 3.6.

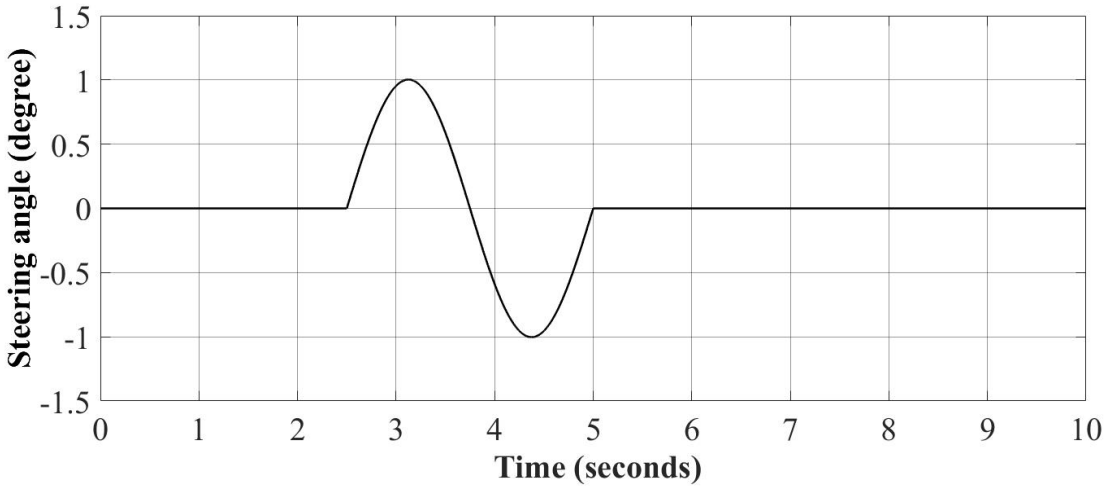

Figure 3.5: Open-loop SLC steering input

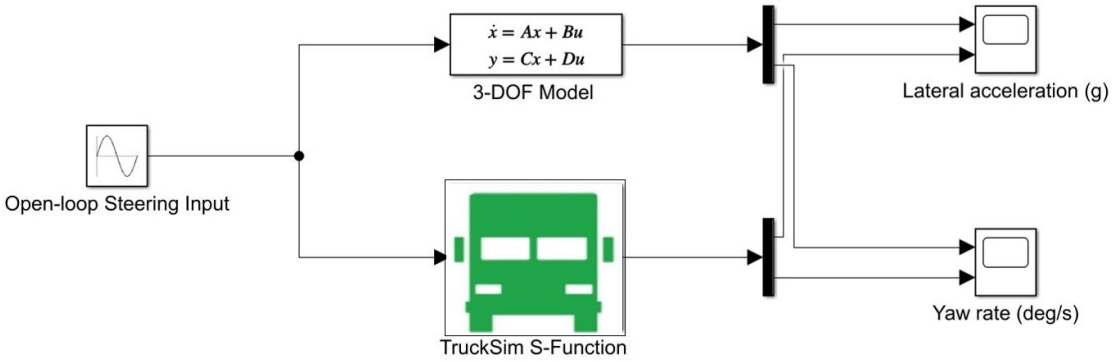

FIGURE 3.6: Block diagram of the open-loop environment for validation

The fidelity of the 3-DOF linear model is established by comparing the lateral acceleration and yaw rate with the pickup truck-trailer configuration in TruckSim. Figures 3.7 and 3.8 depict the lateral acceleration and yaw rate responses of the 3-DOF model and TruckSim.

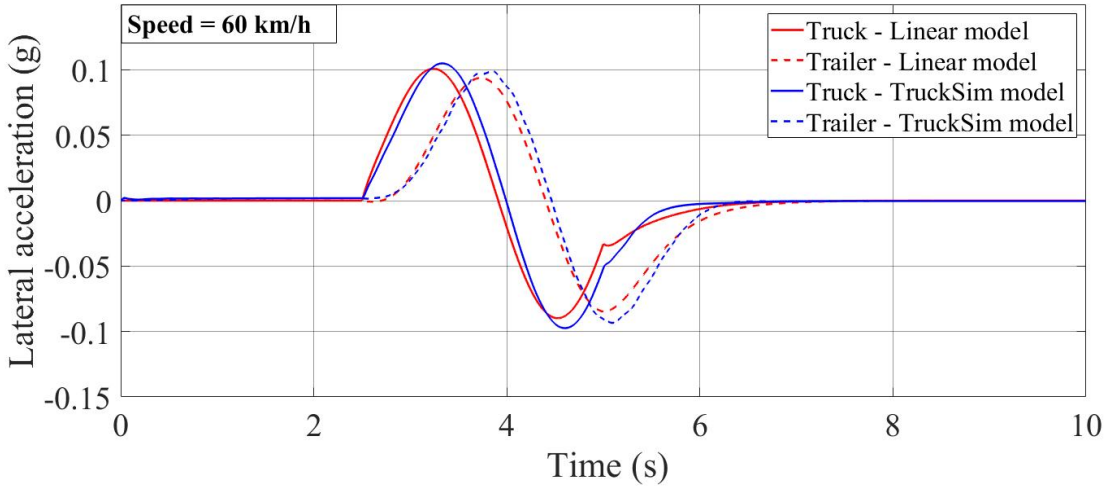

FIGURE 3.7: Lateral acceleration responses of the 3-DOF model and TruckSim model

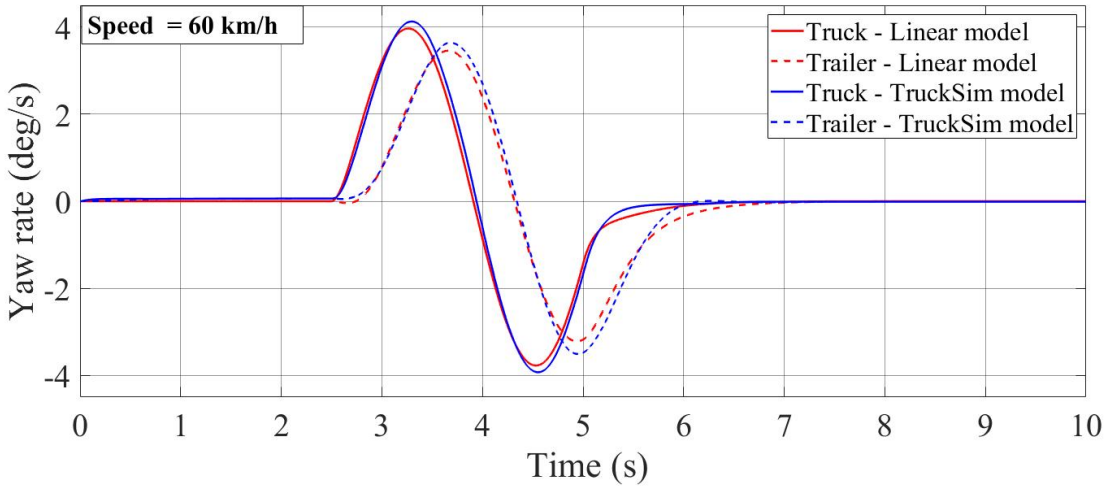

FIGURE 3.8: Yaw rate responses of the 3-DOF model and TruckSim model

The lateral acceleration and yaw rate curves of the 3-DOF linear model demonstrate reasonable agreement with the responses of the TruckSim model. However, a slight variation in the peak values of both lateral accelerations and yaw rates are observed. This variation is attributed to the nonlinearity of the TruckSim model.

Despite the assumptions made, the simplified linear model is a fair representation of the motions in concern for this research.

3.5 Eigenvalue Stability Analysis

System stability is an imperative factor in the design and control of vehicle systems, as it is closely associated with system safety. Eigenvalue stability analysis is performed to determine the stability boundaries of the 3-DOF linear vehicle system developed in Section 3.2. This method aids in the estimation of unstable motion modes and critical speeds of the linear vehicle model. The eigenvalues of the dynamic system are computed using the system matrix A of the 3-DOF linear model [89, 90].

Each pair of the eigenvalue is represented as a complex characteristic root given by:

$$S_{1,2} = R_e \pm j\omega_d \tag{3.9}$$

where, R_e is the real part and $j\omega_d$ is the imaginary part. For a system to be deemed stable, all the roots should have negative real parts. If any pair of the roots have a positive real part, the system is characterized to be dynamically unstable. The real and imaginary parts of equation 3.9, are then used to calculate the damping ratio ζ, as shown in the following equation.

$$\zeta = \frac{-R_e}{\sqrt{(R_e)^2 + (\omega_d)^2}} \tag{3.10}$$

The damping ratio is expressed as a function of vehicle forward speed. A damping ratio of 1 implies that the system is stable. Once the damping ratio approaches zero, the vehicle system is close to instability and in the negative region, the vehicle becomes unstable [89, 90].

In Chapter 2, it was established that trailer parameters have a significant impact on the stability of articulated vehicles. Therefore, the stability of the 3-DOF linear model is assessed under varying trailer parameters, i.e. trailer's payload longitudinal CG distance and weight.

The stability boundaries of the vehicle combination were evaluated at payload weights of 0 kg, 1000 kg, 2000 kg and 3000 kg and longitudinal CG distances of 5 m, 5.5 m and 6 m from the hitch. Parameters such as cornering stiffness and trailer yaw moment of inertia are significantly influenced by the payload, and therefore, these parameters were adjusted accordingly. The rest of the parameters were kept constant, and the damping ratios at various forward speeds were

evaluated. Table 3.1 demonstrates the influence of varying payload weights at constant CGs. The overall behaviour of the system suggests that with increasing payload, the damping ratio tends to reduce, indicating instability of the system at higher payload weights. Close observation of the results indicates the vehicle's vulnerability to unstable motion modes at high speeds, with higher payloads and CG distances located further away from the hitch.

TABLE 3.1: Summary of eigenvalue sensitivity analysis

Case No.	**Weight (kg)**	**CG (m)**	**Damping ratio**					
			Motion Mode 1			**Motion Mode 2**		
			Min	Max	Speed (km/h)	Min	Max	Speed (km/h)
1	0	5	0.289	1	above 200	0.715	1	above 200
2	1000	5	0.27	1	above 200	1	1	above 200
3	2000	5	0.27	1	above 200	-1	1	180
4	3000	5	0.281	1	above 200	-1	1	200
5	0	5.5	0.211	1	above 200	0.594	1	above 200
6	1000	5.5	0.264	1	above 200	0.716	1	above 200
7	2000	5.5	0.295	1	above 200	0.71	1	above 200
8	3000	5.5	0.343	1	above 200	0.57	1	above 200
9	0	6	-0.019	1	200	0.68	1	200
10	1000	6	-0.048	1	180	0.724	1	180
11	2000	6	-0.038	1	180	-0.70	1	180
12	3000	6	-0.639	1	200	0	1	200

3.6 Summary

In this chapter, a 3-DOF yaw-plane model was derived. This model was then validated against a nonlinear pickup truck-trailer model in TruckSim under an open-loop SLC maneuver, to establish the fidelity of the yaw-plane model. The

simulation results demonstrated reasonable agreement between the linear and nonlinear models. Finally, the stability boundaries of the 3-DOF model were determined by carrying out an eigenvalue stability analysis and the effect of varying speeds, trailer's payload weights and CG distances were examined. In subsequent chapters, this 3-DOF linear model is employed to design the ATS systems.

Chapter 4

Design of Active Trailer Steering Controllers

4.1 Introduction

In this chapter, the implementation of the LQR-based and H_∞-based ATS controllers are discussed. Furthermore, the associated control theories and mathematical laws governing these control strategies are elaborated in detail. This section also illustrates the co-simulation environment generated between TruckSim and MATLAB/Simulink, on the basis of which, the dynamic performance of the vehicle is evaluated.

4.2 LQR Control Technique

The LQR controller is a full-state optimal feedback controller. In the design process of LQR, a gain matrix K is calculated based on the state-space model mentioned in section 3.2, to attain the desired system performance.

The LQR problem is defined as a quadratic cost function represented by:

$$J = \int_0^\infty (x^T Q x + u^T R u) dt \tag{4.1}$$

where, Q is the weighting matrix that penalizes the magnitude of the states and R is the weighting matrix that penalizes the control inputs. Both Q and R are represented as a positive-definite matrix.

The optimal control law is determined by minimizing the quadratic cost function (Equation 4.1) and is denoted by:

$$u = -Kx \tag{4.2}$$

where, K is the feedback gain and is computed by solving the Algebraic-Riccati Equations [15, 90].

4.2.1 LQR weighting matrices

The main objective of the controller design is to improve the high-speed lateral behaviour of the pickup truck-trailer combination, in the presence of an external steering input [16]. This objective is achieved by selecting the weighting functions Q and R appropriately. As mentioned earlier, the Q matrix is applied to the states of the system. The desired performance is obtained by penalizing the values in the Q matrix corresponding to the concerned states. R matrix, on the other hand, penalizes the magnitude of control input or actuator effort required to achieve the desired performance. In this study, matrices Q and R are tuned manually to achieve the desired performance.

4.2.2 LQR-based ATS system

The LQR controller described above is utilized to design an ATS system for the pickup truck-trailer combination. Figure 4.1 illustrates a block diagram of the LQR-based ATS system developed in the co-simulation environment with TruckSim and MATLAB/Simulink. The desired ATS angles are generated with the help of the LQR gain matrix obtained using the Control System Toolbox in MATLAB.

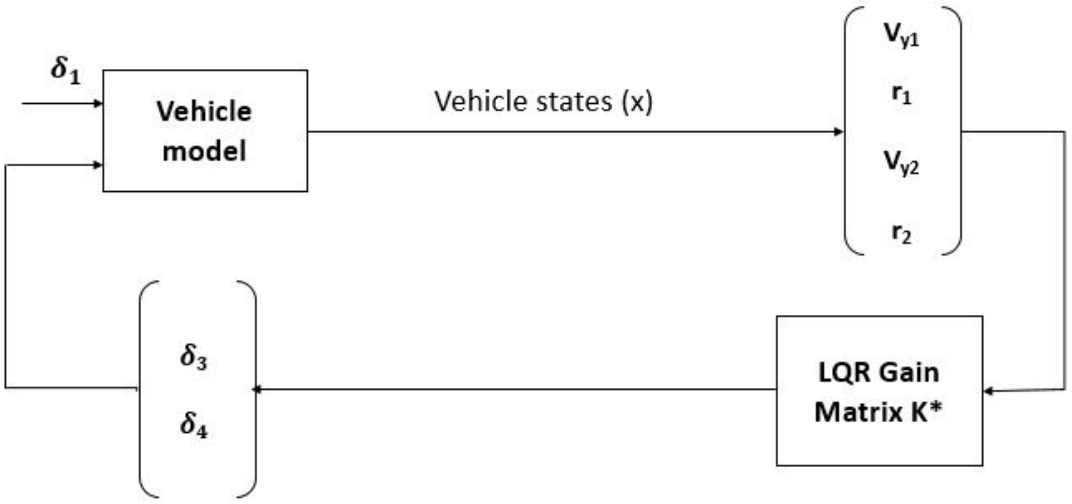

FIGURE 4.1: Schematic representation of the LQR-based ATS controller

4.3 H_∞ Control Technique

The concept of robustness and its importance in control system design has been highlighted extensively in previous studies [1, 12, 15, 18, 64]. The robust control theory assumes that there exists an error between the actual plant and the mathematical model used, and therefore, this error is used in the design process of the control system. In reality, physical systems are complex and highly

vulnerable to external disturbances and operating conditions. In articulated vehicle systems, for example, payload parameters such as weight, the moment of inertia and tire cornering stiffness are constantly prone to variations. These variations affect the dynamic behaviour of the system significantly, which can, in turn, compromise the stability of the vehicle. LQR controllers are generally designed based on perfectly known and pre-defined parameters. Moreover, the LQR controller does not necessarily provide the optimal solution in the presence of parametric uncertainties or external disturbances [16]. Therefore, the robust H_∞ controller is proposed in this study to account for uncertainties, such as the trailer's payload weight and payload's CG distances.

4.3.1 H_∞ control theory

H_∞ control technique is adopted in the design process of the robust ATS controller. The standard H_∞ control layout is illustrated in Figure 4.2. In the figure, G_{aug} is the augmented system, and K is the stabilizing H_∞ controller; ω and z represent the external inputs to the system and the weighted performance outputs respectively; u and y denote the control signal and the output signal respectively.

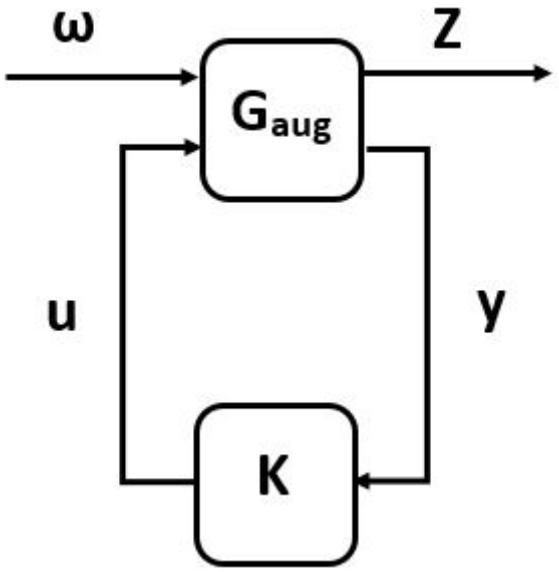

FIGURE 4.2: Standard mixed-sensitivity H_∞ structure [1]

Based on this system, the state-space representation of the augmented plant is given by:

$$\begin{cases} \dot{x} = Ax + B_1\omega + B_2 u \\ z = C_1 x + D_{11}\omega + D_{12} u \\ y = C_y x + D_{y1}\omega + D_{y2} u \end{cases} \tag{4.3}$$

where, x, y, z represent the state, output and weighted output vectors respectively; u and ω denote the control input and external input vectors; A, B_1, B_2, C_1, D_{11}, D_{12}, C_y, D_{y1} and D_{y2} represent the state-space matrices [81].

The objective of the H_∞ control problem is to find a controller, K, that can guarantee both performance and stability of the plant G under parametric uncertainties such as payload weight ranging between 0-3000 kg and its longitudinal CG distance ranging from 5-6 m. The controller K is given by:

$$u = Ky \tag{4.4}$$

and the state-space representation of K is given by:

$$\begin{cases} \dot{\eta} = A_K \eta + B_K y \\ u = C_K \eta + D_K y \end{cases} \tag{4.5}$$

where, η is the state vector of the controller and A_K, B_K, C_K and D_K are the state-space matrices of the controller [81].

The standard H_∞ structure depicted in Figure 4.2 is expanded to form the H_∞ closed-loop feedback system. This layout is illustrated in Figure 4.3.

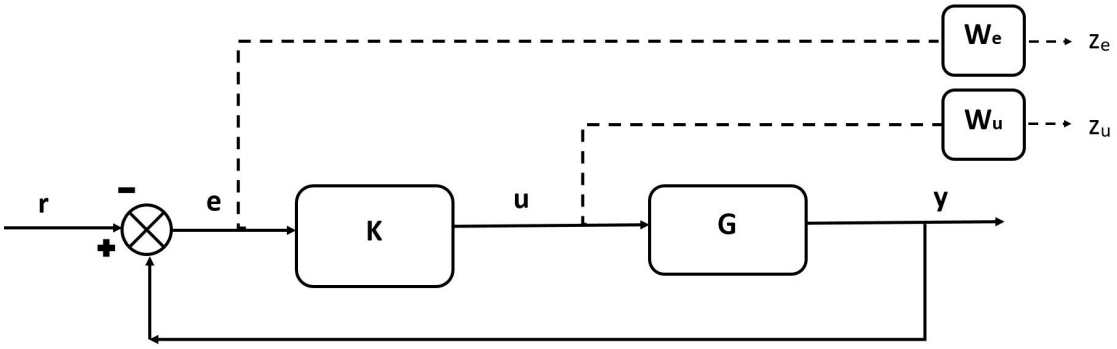

FIGURE 4.3: Mixed-sensitivity H_∞ closed-loop feedback system [1]

where, W_e and W_u represent the weighting functions, the weighted performance output signals are denoted by z_e and z_u, r is the reference signal, e is the error signal, u and y represent the control signal and system output signal vector, G is the uncertain system to be controlled and K is the stabilizing H_∞ controller.

The design objective of a closed-loop system is generally characterized by its cost function. As discussed in Section 4.2, the LQR control technique requires

one cost function. However, the design of an H_∞ controller requires a combination of cost functions for reasonable reference tracking, disturbance attenuation and robust stabilization. The cost function is minimized by employing frequency dependant weighting functions, to achieve the desired controller performance [1, 15, 91]. The cost function of the mixed-sensitivity H_∞ is given in Equation 4.6.

$$min_K \left\| \frac{We(I+GK)^{-}1}{W_u K(I-GK)^{-}1} \right\|_\infty \tag{4.6}$$

This formulation permits proper reference tracking and limits the control signal energy. The design objective of the H_∞ technique is to minimize the output signal for all external inputs by computing the controller feedback gain K [1].

4.3.2 H_∞ weighting functions

Selecting appropriate weighting functions is crucial in attaining the system's desired performance objectives. These weights are the tuning parameters to achieve the best compromise between various objectives. The control system is composed of the performance weighting functions (W_e) and control signal weighting functions (W_u). Similar to the LQR controller, these weighting functions were also manually tuned. The performance weighting functions regulate the yaw rate error output signals, and the control signal weighting functions regulate the magnitude of control input requirements. The weighting functions used in this study are adopted from [12, 92] and have been manually tuned to obtain the desired performance. The weighting functions used in this research are given below:

$$W_{e1} = \frac{0.7879s + 3.072}{s + 0.000181}$$

$$W_{e2} = \frac{0.9138s + 3.203}{s + 0.000181}$$

$$W_{u1} = \frac{0.00225s + 0.001465}{0.009061s + 1}$$

$$W_{u2} = \frac{0.08752s + 0.0171}{0.5092s + 1}$$

4.3.3 Yaw rate reference model

The H_∞ controller requires a suitable reference signal to track the desired yaw rate for the pickup truck-trailer combination. This technique ensures that the vehicle maintains its intended path. The control signal is generated when the controller receives the error between the reference yaw rate signal and the actual yaw rate of the plant. Numerous studies have implemented robust controllers that use yaw rate tracking to enhance the lateral stability of the vehicle [12, 15, 18, 91]. Moreover, yaw rate manipulation directly influences the lateral acceleration of the vehicle [91].

The desired yaw rate is frequently calculated using the linear vehicle model [12, 15, 18, 91]. The steady-state yaw rate of the linear yaw-plane model is considered as the desired yaw rate and is expressed as a function of steering input and vehicle forward speed. In this study, the steady-state yaw rate is obtained using the linear vehicle model presented in Section 3.2 at steady-state conditions. The steady-state yaw rate of the pickup truck towing a tandem-axle

trailer is represented by [89]:

$$r_{ss} = \frac{U}{L + k_{us} U^2} \delta \tag{4.7}$$

where, r_{ss} is the steady-state yaw rate of the pickup truck, U is the constant forward speed and δ is the steering input. The parameter L is given by:

$$L = \frac{l_1 - C_3 C_4 {l_2}^2 [C_1(l_1 + (d-b)) + C_2(d-b)]}{C_1 C_2 l_1 [C_3(e+f) + C_4(l_2 + (e+f)]} \tag{4.8}$$

where, $l_1 = a + b$ and $l_2 = g - f$. The understeer coefficient k_{us} of the pickup truck is given by:

$$k_{us} = \frac{m_1 a_g}{l_1}(\frac{b}{C_1} - \frac{a}{C_2}) - \frac{m_2 a_g (C_4 g - C_3 f)[C_1(l_1 + (d-b)) + C_2(d-b)]}{C_1 C_2 l_1 [C_3(e+f) + C_4(l_2 + (e+f))} \tag{4.9}$$

where, a_g is the acceleration due to gravity. The rest of the parameters are described in the Appendix.

Appropriate time and transport delays are then added to the system to achieve the desired yaw rates of each of the vehicle units [12, 15, 91]. The desired yaw rate is presented below:

$$r_{desired} = (\frac{1}{1 + \tau_{delay} s}) r_{ss} \tag{4.10}$$

where, $r_{desired}$ is the desired yaw rate and τ_{delay} is the induced time-delay.

Finally, the desired yaw response is bounded by a function of road adhesion coefficient presented by [93] and implemented by [15, 91, 94]. The bounded

yaw response is depicted by:

$$r_{desired,bound} = \mid 0.85 \frac{\mu a_g}{U} \mid \tag{4.11}$$

where, μ is the road adhesion coefficient and a_g is the acceleration due to gravity. When the desired yaw rate exceeds the bounded yaw response, the value is saturated to $\pm r_{desired,bound}$.

4.3.4 H_∞-based ATS system

In this study, a robust H_∞ controller is used to design the ATS system, that is capable of attaining robust stability by considering parameter variations. Moreover, H_∞ ensures superior yaw rate tracking of the vehicle units.

The configuration of the H_∞-based ATS system is illustrated in Figure 4.4, where the performance weighting function, W_e, tailors the yaw rates, r_1, r_2, of the pickup truck and trailer and the control weighting function, W_u, characterizes the ATS angles, δ_3, δ_4. The configuration in [15] was modified to match the requirements of the proposed control system. The H_∞-based ATS controller is obtained using the Robust Control Toolbox in MATLAB. The external input to the system δ_1 is the steering angle input that is fed to the vehicle model and reference model. The performance signals are denoted by the error tracking signal for the pickup truck, z_{e1}, and trailer, z_{e2}, and two control signal attenuation signals, z_{δ_3} and z_{δ_4}. Each of the performance signals is weighted by a unique weighting function, as mentioned in Section 4.3.2. The inputs y to the H_∞ controller are the error signals between the reference yaw rates and the actual yaw rates. The controller's outputs u are the ATS angles, δ_3 and δ_4.

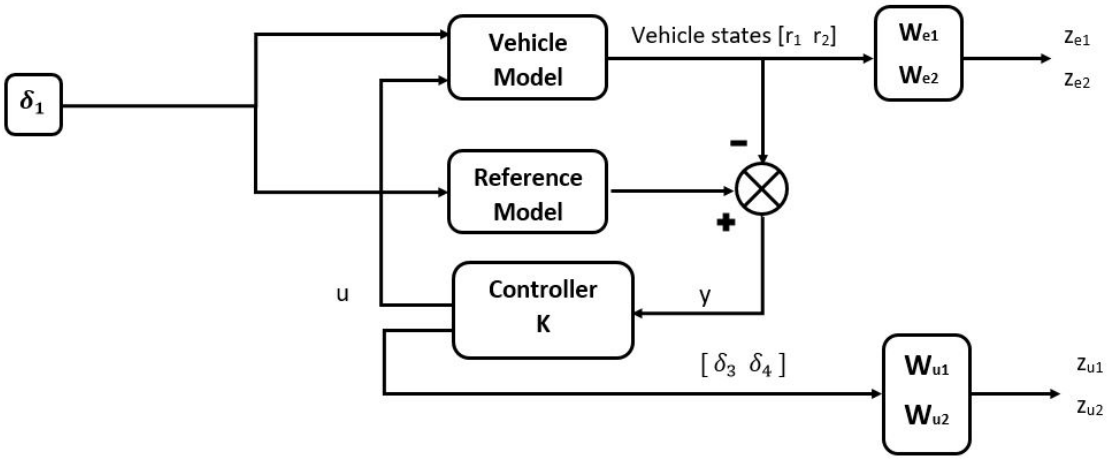

FIGURE 4.4: Schematic representation of the H_∞-based ATS controller

4.4 Summary

The LQR and H_∞ control theories were introduced in this chapter for the design of ATS systems. Additionally, the theoretical steps involved in the design of the LQR and H_∞-based ATS systems were discussed. The objective of the LQR controller is achieved by appropriately tuning the weighting matrices Q and R, using the method of trial and error. The performance and control weighting functions of the H_∞ controller are tuned similarly. Moreover, the reference yaw rate model used by the H_∞ controller to facilitate reference tracking is also discussed. This yaw rate model is crucial for the enhanced dynamic performance of the pickup truck-trailer combination.

Chapter 5

Case Study: Extreme Case Scenario

In this chapter, an extreme case scenario is introduced to investigate the dynamic behaviour of a pickup truck-trailer configuration under extreme conditions. The configuration is subjected to loads based on the maximum towing capacity and maximum rear axle loads of the pickup truck and maximum allowable payload height. Two configurations with different trailer parameters are investigated in the following sections.

5.1 Configuration I

The extreme case scenario is based on a study carried out in [27], where the dynamic performance of seven different pickup truck-trailer configurations were evaluated. The Class 2 pickup truck and gooseneck trailer configuration is referred to as Configuration I. The parameters of the pickup truck models were based on data sheets published by the Original Equipment Manufacturer (OEM). The trailer and payload specifications were based on Commercial Vehicle Safety and Enforcement (CVSE) policies, maximum towing capacity and

maximum rear axle loads of the pickup truck. Furthermore, the payload CG height was based on the maximum legal overall height in British Columbia, Canada. The CG height of the payload (PH) is determined using the equation below:

$$PH = \frac{MH - TDH}{2} + TDH \tag{5.1}$$

where, MH is 4.15 m, and it is the maximum legal overall height for vehicles in British Columbia. TDH represents the trailer deck height.

The performance measures used in this study are adopted by CVSE to aid in the development of safety regulations related to the stability of articulated vehicles. In the following sections, the dynamic behaviour of Configuration I, under the standard high-speed maneuvers described in Chapter 1.3, is presented:

5.1.1 Steady-state ramp-steer maneuver

As described in Section 1.3, the handling characteristics and SRT are determined at steady-state by the application of a ramp-steer input. Based on the standards specified in [27, 28], the configuration is evaluated under a ramp-steer input of 1.33 deg/s at a constant forward speed of 90 km/h. The maneuver is depicted in Figure 5.1.

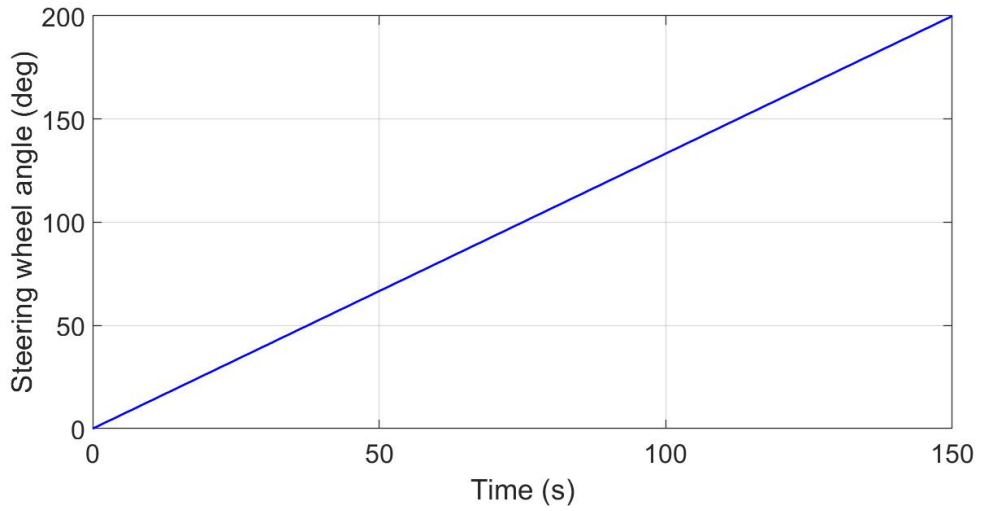

FIGURE 5.1: Ramp-steer maneuver

The performance measures based on the maneuver mentioned above are described below:

1. Handling performance: This measure is evaluated based on the construction of a handling diagram illustrated in Figure 5.2. The x-axis represents the parameter $\frac{Lr}{U} - \frac{\delta}{N_g}$ and the y-axis represents the lateral acceleration in g-units. The understeer coefficient is the negative inverse of the slope in Figure 5.2 at a particular value of lateral acceleration. From the figure, it is apparent that the configuration exhibits understeer characteristics.

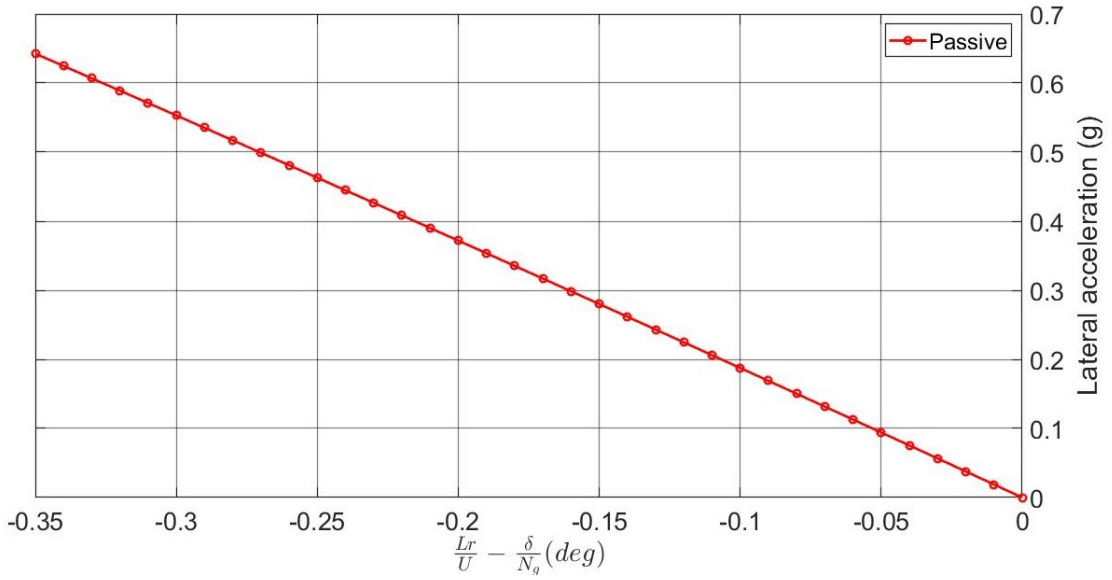

FIGURE 5.2: Handling diagram of Configuration I

Table 5.1 portrays the pass/fail criteria based on the three-point measure described in Section 1.3.2.1.

TABLE 5.1: Configuration I handling performance - Pass/Fail benchmark

Points	**Units**	**Benchmark**	**Configuration I**
Point 1 (Transition)	g	≥ 0.20 g	Pass
Point 2 (0.3 g)	deg/g	≥ -3.31 deg/g	0.55 - Pass
Point 3 (0.1 g)	deg/g	0 - 2 deg/g	0.57 - Pass

2. Static Rollover Threshold (SRT): The SRT is determined by measuring the lateral acceleration at which the last axle of the configuration just lifts off the ground. Figure 5.3 illustrates the scenario on the basis of which the SRT is computed.

FIGURE 5.3: Rollover prediction for Configuration I

Table 5.2 represents the pass/fail benchmark used to assess the SRT of Configuration I.

TABLE 5.2: Configuration I SRT - Pass/Fail benchmark

Measure	**Units**	**Benchmark**	**Configuration I**
SRT	g	$\geq$ 0.4 g	0.64 g - Pass

5.1.2 SLC maneuver

The SLC maneuver specified in [27] is illustrated in Figure 5.4 and is performed at a constant forward speed of 88 km/h. This maneuver is applied to evaluate the following performance measures.

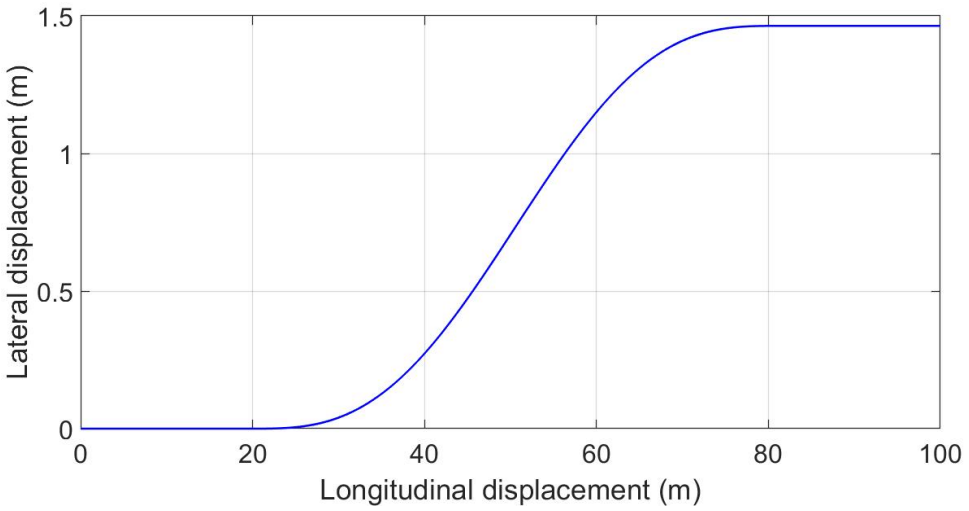

FIGURE 5.4: SLC maneuver

1. RWA ratio: The RWA ratio is the ratio of the maximum (absolute value) lateral acceleration at the CG of the trailer to that of the leading unit. Figure 5.5 represents the time history of lateral accelerations of both the units in Configuration I. The pass/fail benchmark used to assess this measure is provided in Table 5.3.

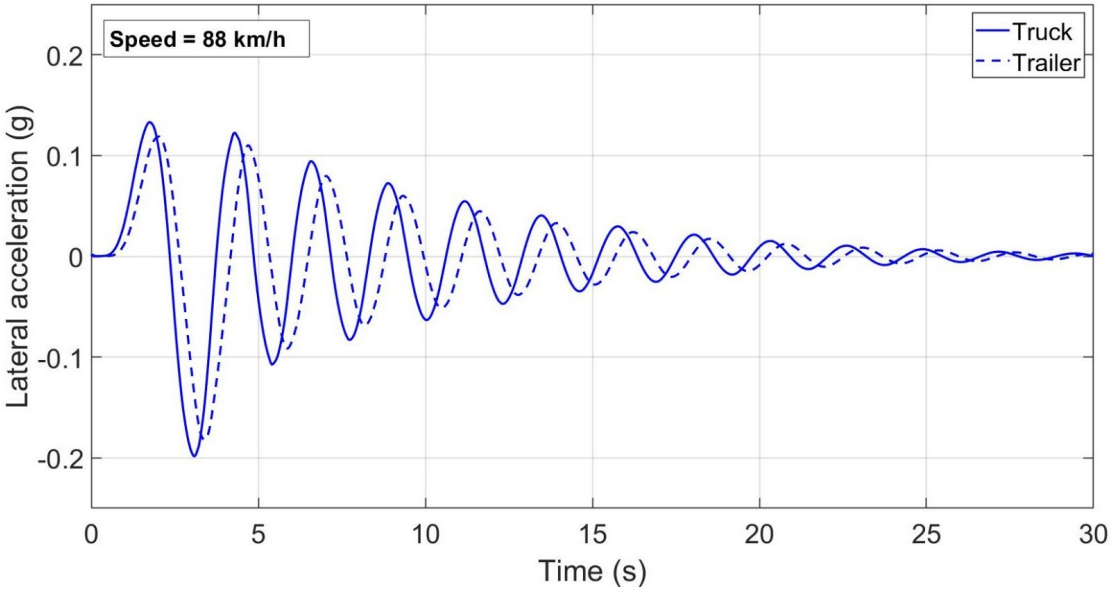

FIGURE 5.5: Lateral acceleration responses of Configuration I

2. LTR: The LTR is determined to evaluate the load transfer between the left and right tires, which causes a variation in the left and right normal forces. It is calculated using the formula presented in Section 1.3.1.2. The pass/fail benchmark used to assess this measure is provided in Table 5.3.

3. Offtracking: Offtracking is characterized as the deviation of the rearmost axle with reference to the path taken by the first axle, which is also known as the overshoot. Figure 5.6 illustrates the lateral displacement of axles 1 and 4. The pass/fail benchmark used to assess this measure is provided in Table 5.3.

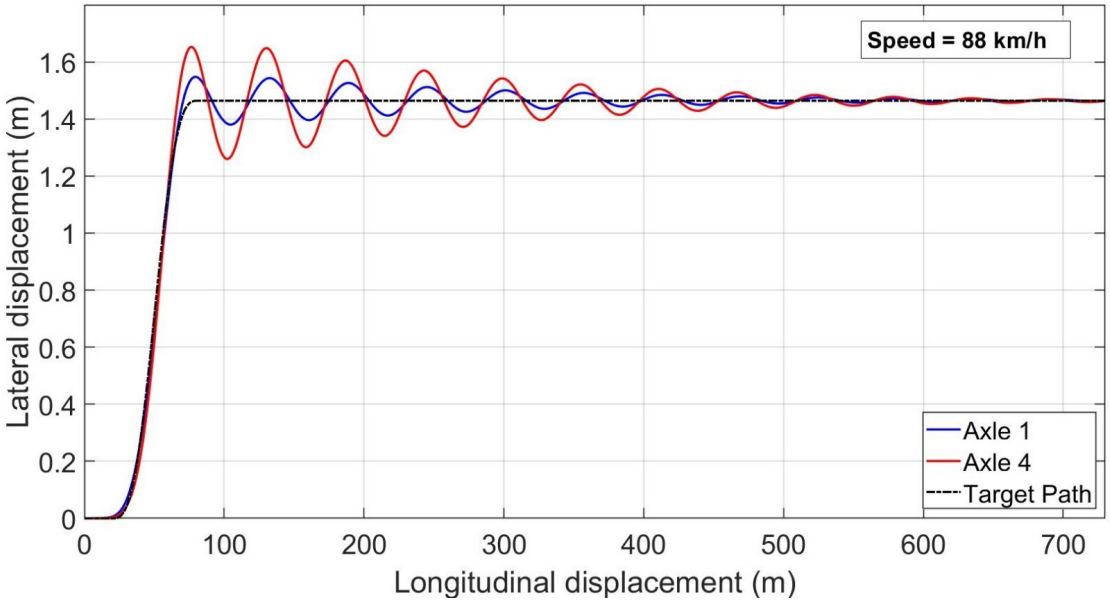

FIGURE 5.6: Offtracking for Configuration I

TABLE 5.3: Performance measures under an SLC maneuver for Configuration I - Pass/Fail benchmark

Measure	**Units**	**Benchmark**	**Configuration I**
RWA ratio	N/A	≤ 2	0.92 - Pass
LTR	N/A	≤ 0.6	0.24 - Pass
Offtracking	m	≤ 0.8	0.25 - Pass

5.1.3 Discussion

Analyzing the results obtained above, it was observed that although it passed all the performance benchmarks, Configuration I was significantly unstable and experienced high oscillations (refer Figures 5.5 and 5.6). This is attributed to trailer's parameters such as the location of trailer's hitch on the bed of the pickup truck and trailer's longitudinal CG distance. In this configuration, the trailer's hitch was located slightly ahead of the pickup truck's rear axle. Additionally, the longitudinal CG distance was located closer to the hitch of the trailer.

Therefore, in order to obtain a reasonably stable configuration, a gooseneck trailer based on the standard TruckSim model, with a longitudinal CG distance further away from the hitch, is proposed. Moreover, the trailer's hitch is placed directly above the pickup truck's rear axle. More details on the trailer parameters are provided in the Appendix. The Class 2 pickup truck combined with this trailer will be referred to as Configuration II, and its dynamic behaviour at high speeds is evaluated in the following section.

5.2 Configuration II

In this section, Configuration II is evaluated under the same test conditions described in Section 5.1. To further investigate the performance of Configuration II, the payload's longitudinal CG distance locations are placed at two different points, i.e. 5 m and 6 m from the trailer's hitch.

In the following subsections, along with the dynamic behaviour of the passive Configuration II, the effect of applying LQR-based and H_∞-based ATS controllers to the configuration is investigated.

5.2.1 Steady-state ramp-steer maneuver

Based on the maneuver described in Section 5.1.1, Configuration II is evaluated on the following performance measures.

1. Handling performance:

   (a) **Payload longitudinal CG distance of 5 m:** Figure 5.7 represents the handling diagram of Configuration II with a payload longitudinal CG distance of 5 m. The diagram illustrates the handling characteristics of Configuration II in passive state and with the application of LQR and H_∞-based ATS controllers. From the figure, it is apparent that the configuration exhibits oversteer characteristics in passive state and understeer characteristics in active states. Table 5.4 portrays the pass/fail criteria of the configuration in passive state and with the application of LQR and H_∞-based ATS controllers.

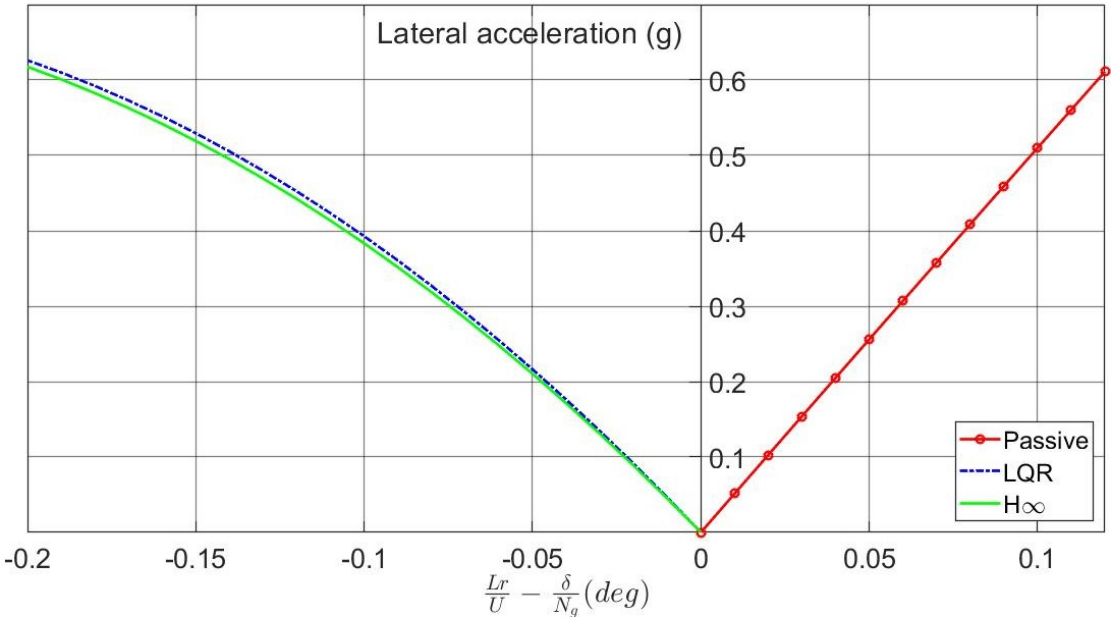

FIGURE 5.7: Handling diagram of Configuration II (5 m payload CG)

TABLE 5.4: Configuration II (5 m payload CG) handling performance - Pass/Fail benchmark

Points	**Units**	**Benchmark**	**Configuration I**		
			Passive	LQR	H_∞
Point 1 (Transition)	g	≥ 0.20	Fail	Pass	Pass
Point 2 (0.3 g)	deg/g	≥ -3.31	-0.2132 Pass	0.2710 Pass	0.2838 Pass
Point 3 (0.1 g)	deg/g	0 - 2	-0.2478 Fail	0.2269 Pass	0.2300 Pass

(b) **Payload longitudinal CG distance of 6 m:** Figure 5.8 depicts the handling diagram of Configuration II with a payload longitudinal CG distance of 6 m. The handling behaviour observed in this case is similar to the behaviour observed at a payload longitudinal CG distance of 5 m.

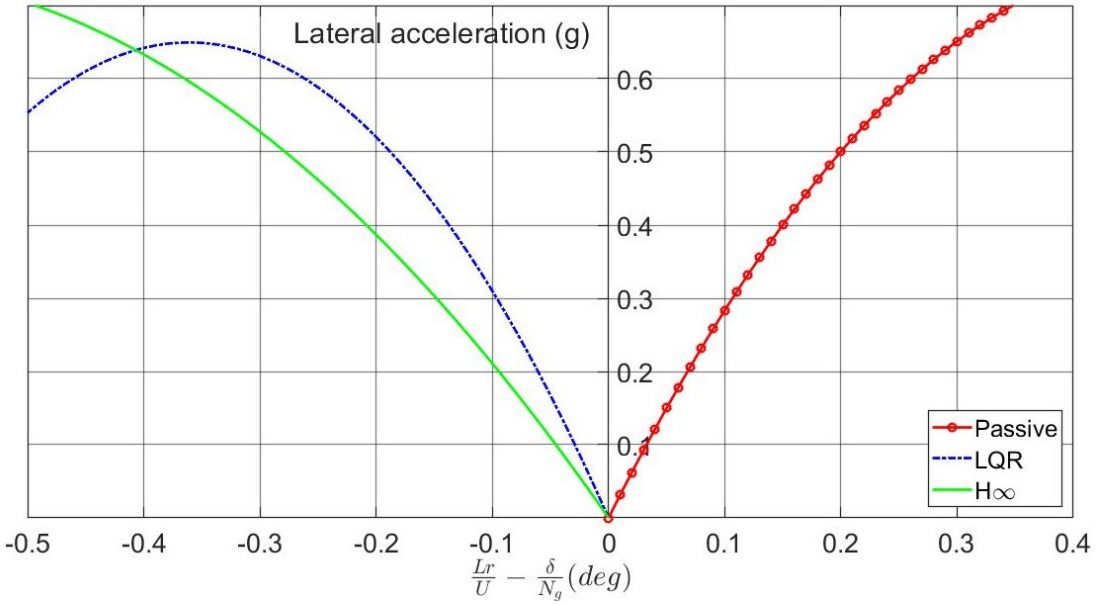

FIGURE 5.8: Handling diagram of Configuration II (6 m payload CG)

TABLE 5.5: Configuration II (6 m payload CG) handling performance - Pass/Fail benchmark

Points	**Units**	**Benchmark**	**Configuration I**		
			Passive	LQR	H_∞
Point 1 (Transition)	g	≥ 0.20	Fail	Pass	Pass
Point 2 (0.3 g)	deg/g	≥ -3.31	-0.4211 Pass	0.3816 Pass	0.5570 Pass
Point 3 (0.1 g)	deg/g	0 - 2	-0.4094 Fail	0.3006 Pass	0.4607 Pass

2. Static Rollover Threshold (SRT): The SRT of Configuration II with payload longitudinal CG distances of 5 m and 6 m, under both passive and active states are demonstrated in Table 5.6.

TABLE 5.6: Configuration II SRT - Pass/Fail benchmark

Payload CG distance	**Measure**	**Unit**	**Benchmark**	**Configuration II**		
				Passive	LQR	H_∞
5 m	SRT	g	≥ 0.4 g	0.67 Pass	0.65 Pass	0.69 Pass
6 m				0.69 Pass	0.68 Pass	0.71 Pass

5.2.2 SLC maneuver

Based on the SLC maneuver described in Section 5.1.2, Configuration II is evaluated on the basis of its RWA ratio, LTR and offtracking.

1. RWA ratio: Figures 5.9 and 5.10 represent the lateral acceleration responses of both the units in Configuration II with payload longitudinal CG distances of 5 m and 6 m, under both passive and active states. The pass/fail of Configuration II with payload longitudinal CG distances of 5 m and 6 m, under both passive and active states are specified in Tables 5.7 and 5.8.

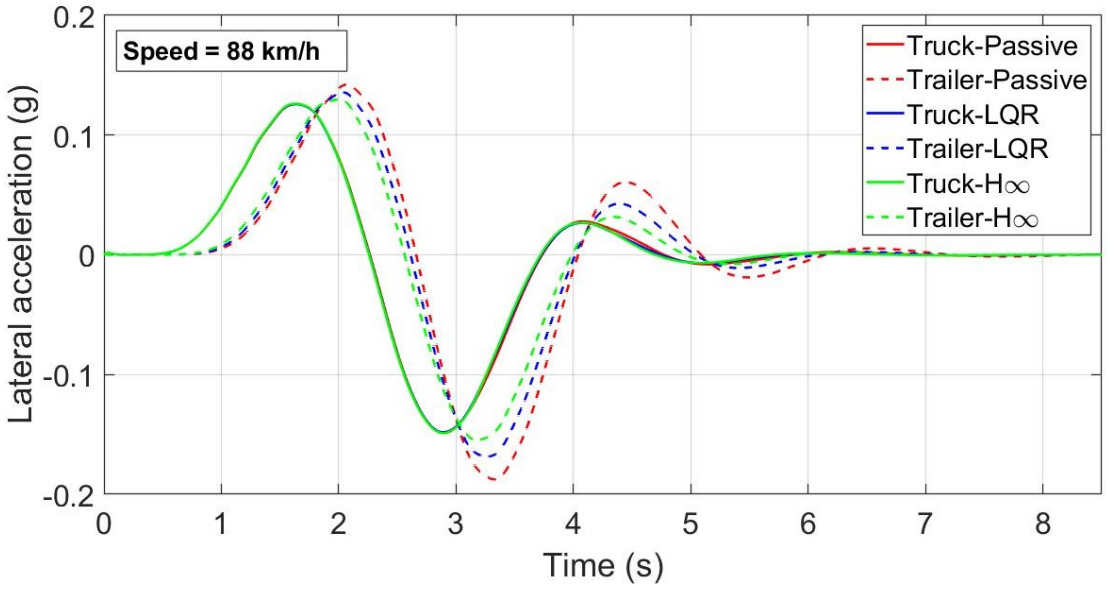

FIGURE 5.9: Lateral acceleration responses of Configuration II under passive, LQR-based ATS and H_∞-based ATS (5 m payload CG)

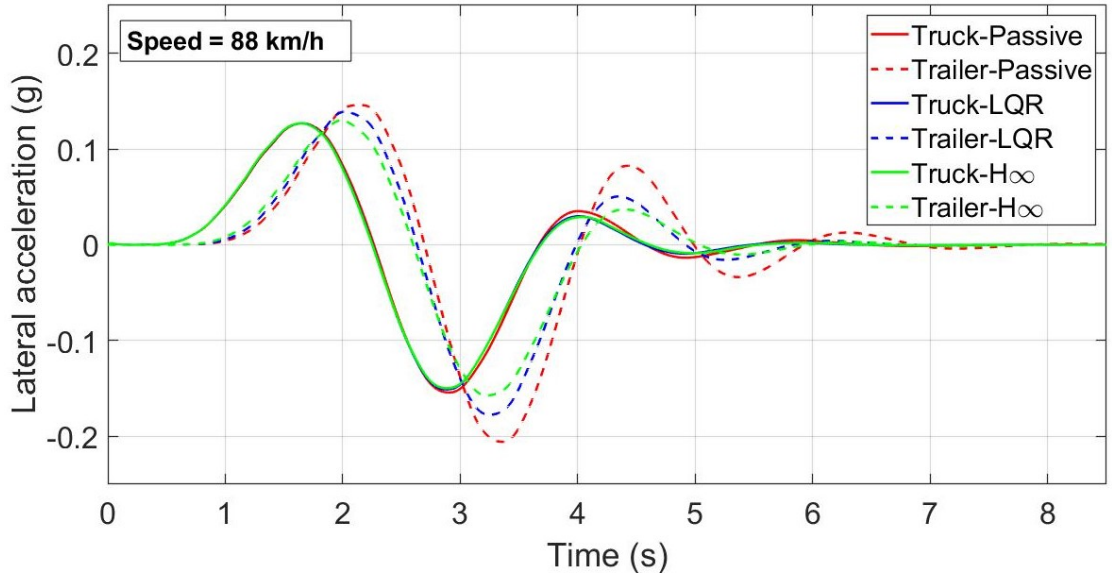

FIGURE 5.10: Lateral acceleration responses of Configuration II under passive, LQR-based ATS and H_∞-based ATS (6 m payload CG)

2. LTR: The pass/fail of Configuration II with payload longitudinal CG distances of 5 m and 6 m, under both passive and active states are specified in Tables 5.7 and 5.8.

3. Offtracking: Figures 5.11 and 5.12 illustrate the lateral displacements of axles 1 and 4 of Configuration II with payload longitudinal CG distances of 5 m and 6 m, under both passive and active states. The pass/fail of Configuration II with payload longitudinal CG distances of 5 m and 6 m, under both passive and active states are specified in Tables 5.7 and 5.8.

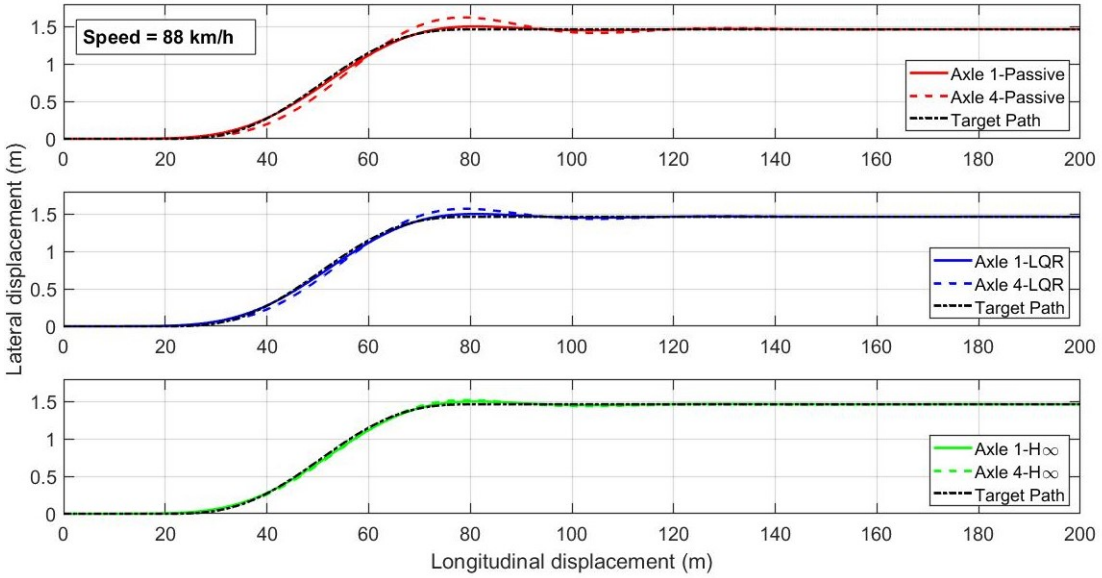

FIGURE 5.11: Offtracking for Configuration II under passive, LQR-based ATS and H_∞-based ATS (5 m payload CG)

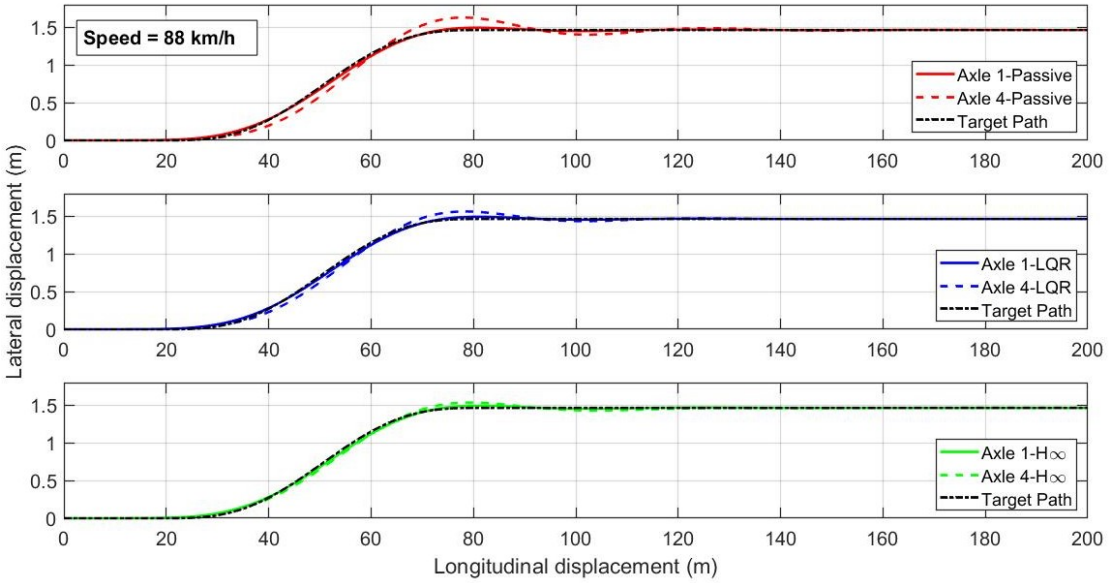

FIGURE 5.12: Offtracking for Configuration II under passive, LQR-based ATS and H_∞-based ATS (6 m payload CG)

TABLE 5.7: Performance measures under an SLC maneuver for Configuration II (5 m payload CG distance) - Pass/Fail benchmark

Measure	**Unit**	**Benchmark**	**Configuration II**		
			Passive	LQR	H_∞
RWA ratio	N/A	≤ 2	1.260 - Pass	1.136 - Pass	1.038 - Pass
LTR	N/A	≤ 0.6	0.221 - Pass	0.204 - Pass	0.192 - Pass
Offtracking	m	≤ 0.8	0.159 - Pass	0.107 - Pass	0.056 - Pass

TABLE 5.8: Performance measures under an SLC maneuver for Configuration II (6 m payload CG distance) - Pass/Fail benchmark

Measure	**Unit**	**Benchmark**	**Configuration II**		
			Passive	LQR	H_∞
RWA ratio	N/A	≤ 2	1.334 - Pass	1.176 - Pass	1.051 - Pass
LTR	N/A	≤ 0.6	0.237 - Pass	0.193 - Pass	0.188 - Pass
Offtracking	m	≤ 0.8	0.165 - Pass	0.099 - Pass	0.071 - Pass

5.2.3 Discussion

The performance measures described in Chapter 1.3 are applied to Configuration II, which is considered as an extreme case scenario in this research. The extreme case indicates that the pickup truck is subjected to extreme loading conditions based on its maximum towing capacity, maximum rear axle loads and maximum legal overall height in British Columbia, Canada.

From the results obtained above, it is observed that in terms of handling characteristics, the configuration exhibits oversteer characteristics at both the conditions of 5 m and 6 m payload longitudinal CG distances. However, on the application of ATS-based controllers, the configuration exhibits understeer characteristics. The configuration with the H_∞-based ATS controller displayed higher understeer behaviour than the configuration with the LQR-based ATS controller. The tendency of the passive configuration to oversteer is attributed mainly to the placement of the trailer's hitch directly above the pickup truck's rear axle. Configuration II exhibits stability and minimal oscillations, as shown in Figures 5.9 - 5.12.

5.3 Summary

In this chapter, an extreme case scenario is evaluated based on a study carried out in [27]. The high-speed performance characteristics of Configuration I were evaluated on the basis of standard performance measures. It was observed that this configuration exhibited instabilities and oscillations at high speeds. In order to address this concern, Configuration II was proposed. To further evaluate the dynamic characteristics of this configuration at high speeds,

the standard performance measures were employed. Additionally, the effect of applying LQR-based and H_∞-based ATS controllers to the configuration was investigated.

Chapter 6

Results and Discussions

6.1 Introduction

An ATS system for a pickup truck-trailer combination was designed using LQR and H_∞ controllers, based on the linear 3-DOF model developed and validated in Chapter 3. The performance of the controllers were evaluated using numerical simulations under different operating parameters, such as trailer's payload weights and payload's longitudinal CG distances. The dynamic responses of the combination vehicle, both with and without control system, were analyzed under a closed-loop SLC maneuver as specified in ISO 14791 [24]. The controllers were evaluated using TruckSim in which a virtual driver is used to follow the prescribed path. The maneuver, depicted in Figure 6.1, determines the desired path to be followed by the vehicle. In this analysis, the performance of the vehicle was evaluated at a constant forward speed of 100 km/h.

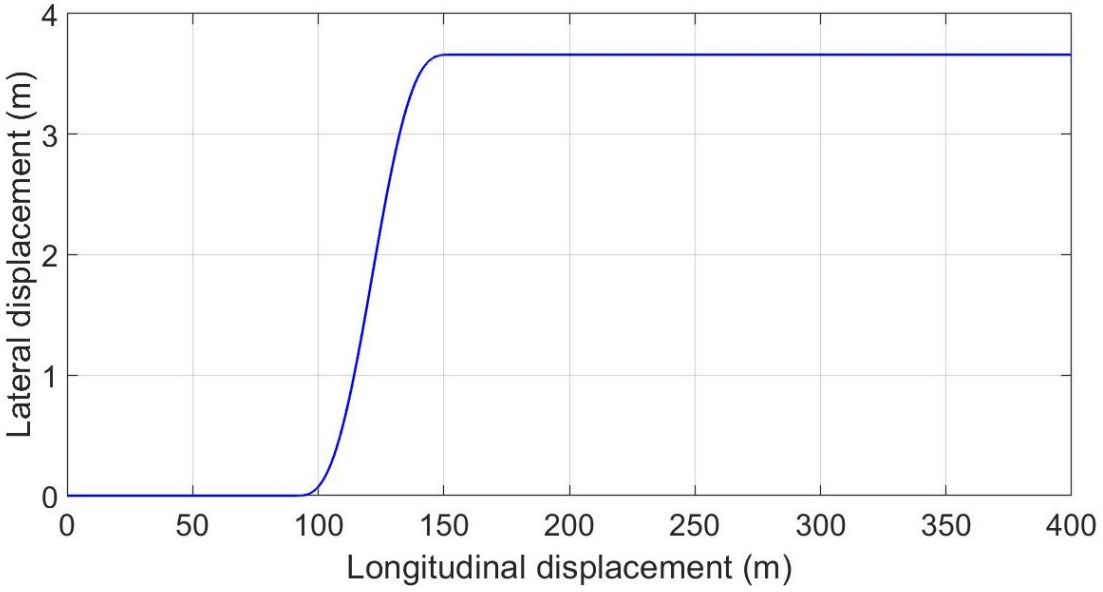

FIGURE 6.1: Closed-loop SLC maneuver

Literature suggests that the dynamic behaviour of an articulated vehicle during a rapid SLC maneuver, is assessed based on three main performance measures namely, RWA ratio, LTR and offtracking [28, 95]. These safety related measures determine the vehicle's tendency to exhibit instabilities such as rollover and trailer sway during high-speed transient maneuvers. Therefore, the performance of the vehicle combination with the incorporated LQR-based and H_∞-based ATS systems were evaluated using these performance measures under varying trailer's payload weights and payload's longitudinal CG distances. The payload weights were varied from 0 kg to 3000 kg, with an increment of 1000 kg. The minimum distance of the payload from the hitch is 5 m, while the maximum is 6 m. Figure 6.2 illustrates the minimum and maximum payload CG distances considered in this study. Table 6.1 portrays the 12 cases evaluated in this study.

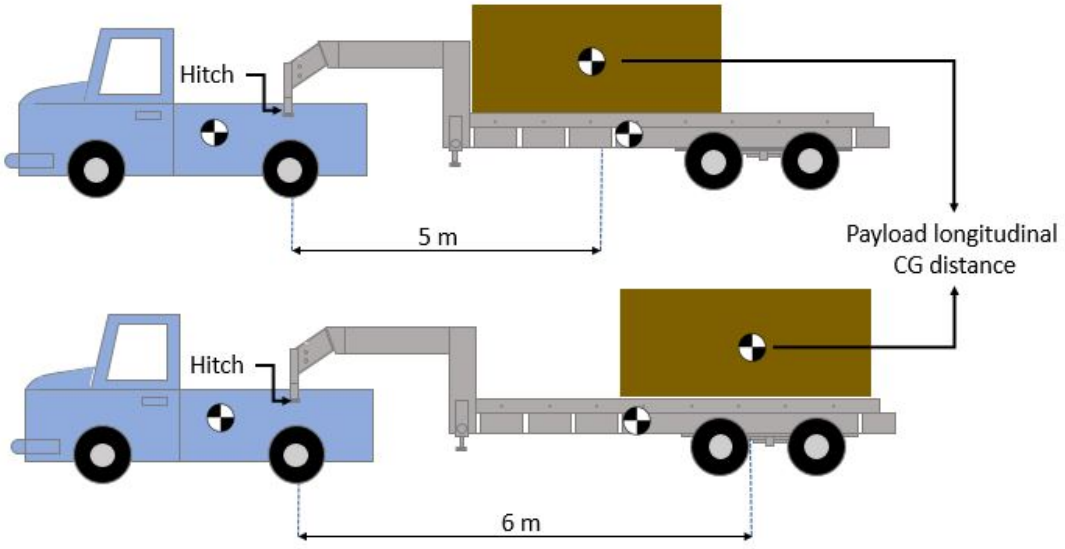

FIGURE 6.2: Minimum and maximum payload CG distances considered in this study

TABLE 6.1: Test cases comprising of varying payloads and CG distances

Case No.	Weight (kg)	Payload CG (m)
1	0	5
2	1000	5
3	2000	5
4	3000	5
5	0	5.5
6	1000	5.5
7	2000	5.5
8	3000	5.5
9	0	6
10	1000	6
11	2000	6
12	3000	6

6.2 LQR-based ATS Controller

6.2.1 Simulation Results

As described earlier, LQR is an optimal controller that utilizes the weighting matrices Q and R to achieve the desired performance of the ATS control system. The weighting matrices were manually fine-tuned based on pre-defined operating parameters such that vehicle combination exhibited improved lateral dynamics. The vehicle combination evaluated is Case 3 from Table 6.1. It comprises of a pickup truck towing a gooseneck trailer with a payload of 2000 kg and the longitudinal CG distance of the payload from the hitch is 5 m. The LQR-controlled vehicle was evaluated under the aforementioned closed-loop SLC maneuver and the results obtained are illustrated in Figures 6.3 - 6.5.

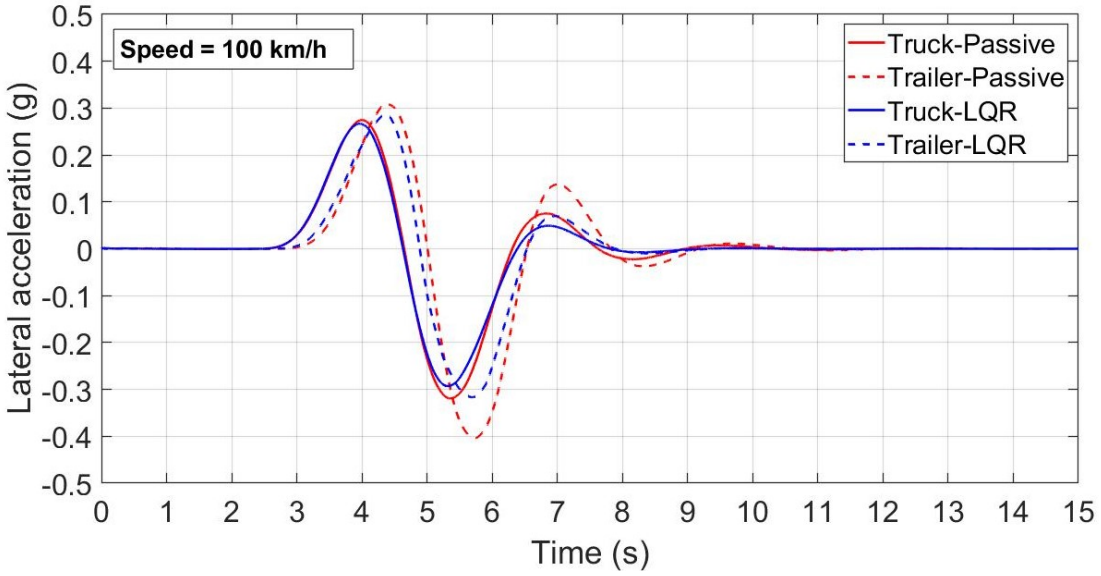

FIGURE 6.3: Lateral acceleration responses for the Case 3 TruckSim model with and without the LQR-based ATS

Figure 6.3 depicts the lateral acceleration responses of the passive TruckSim vehicle and the LQR-controlled vehicle respectively. It is observed that the LQR

controller effectively reduced the peak lateral accelerations of both the pickup truck and trailer, thereby improving the lateral stability of the vehicle.

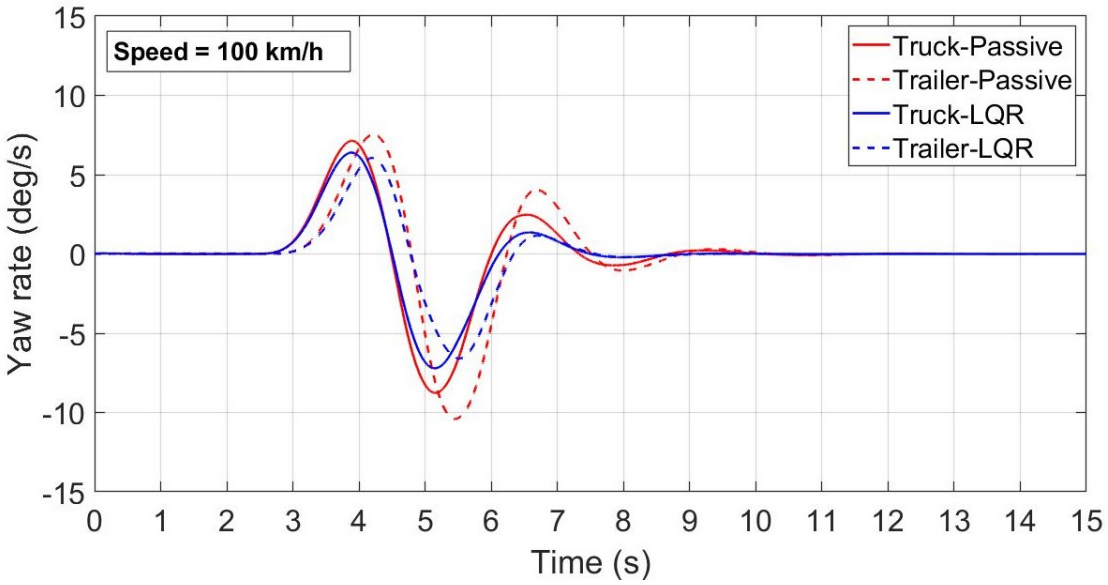

FIGURE 6.4: Yaw rate responses for the Case 3 TruckSim model with and without the LQR-based ATS

Figure 6.4 illustrates the yaw rate responses of the TruckSim baseline vehicle and the LQR-controlled vehicle respectively. The LQR controller also demonstrated superior performance in terms of peak yaw rate reduction of both the units. It is also noteworthy to mention that, the LQR-controlled vehicle displays lower settling time in its yaw rate responses as compared to those of the passive model.

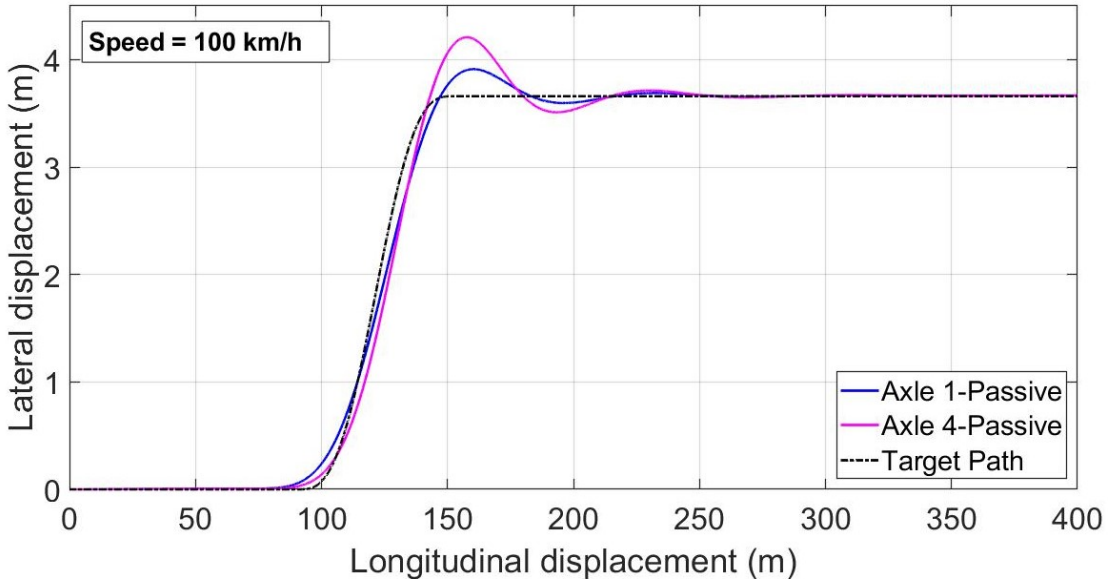

(a)

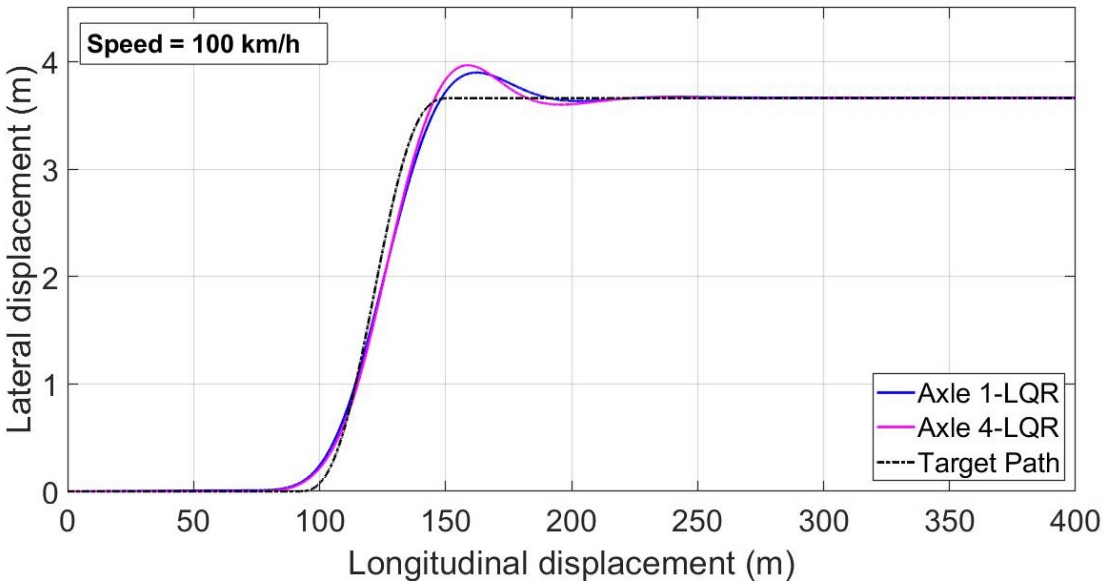

(b)

FIGURE 6.5: Trajectories of axles 1 and 4 of the Case 3 TruckSim model (a) without and (b) with LQR-based ATS

Figure 6.5 indicates the trajectories followed by axles 1 and 4 of the pickup truck-trailer combination. From the figure, it is evident that the lateral displacement of axle 4 from the intended path is far less for the vehicle with the

LQR-based ATS than it is without.

TABLE 6.2: Performance evaluation of the Case 3 TruckSim model with and without the LQR-based ATS system

Payload weight (kg)	**CG distance (m)**	**RWA ratio**		**LTR**		**Offtracking (m)**	
		Passive	LQR	Passive	LQR	Passive	LQR
2000	5	1.267	1.081	0.326	0.265	0.543	0.302

The dynamic performances of the vehicle combination with and without the ATS-based control system were further evaluated under performance measures such as RWA, LTR and offtracking. Table 6.2 presents a summary of the values obtained for RWA, LTR and offtracking. In terms of RWA, an improvement of 21.7% was recorded after the application of the LQR-based ATS system. As mentioned earlier, an RWA ratio of 1 indicates an ideal scenario in which the trailer exhibits the same lateral acceleration as that of the leading unit. An RWA value of 1.081 indicates reduced lateral motions of the trailer during the evasive SLC maneuver. The LTR was found to have improved by 18.7%. Finally, the LQR-based system exhibited favourable offtracking with an improvement of 44.38%.

6.2.2 Drawbacks of LQR Controller

The LQR controller designed in Section 6.2.1 was applied to different cases under varying operating parameters. Table 6.3 illustrates the various cases on which the LQR-based ATS system was applied along with the recorded values of RWA, LTR and offtracking. Case 3 represents the scenario on the basis of which the weighting matrices of the LQR control system were tuned. Without re-tuning the controller, it was applied to the remaining 11 cases described in

Table 6.3. From the table, it is observed that in all the other 11 cases, the RWA, LTR, and offtracking values have reduced with the LQR-based controller.

TABLE 6.3: Performance evaluation of the TruckSim model with and without the LQR-based ATS control system at constant CG distances and varying payload weights

Case No.	**Weight (kg)**	**CG (m)**	**RWA**		**LTR**		**Offtracking (m)**	
			Passive	LQR	Passive	LQR	Passive	LQR
1	0	5	1.315	1.257	0.277	0.203	0.472	0.436
2	1000	5	1.274	1.211	0.276	0.265	0.504	0.440
3	2000	5	1.267	1.081	0.326	0.265	0.543	0.302
4	3000	5	1.269	1.201	0.365	0.350	0.580	0.495
5	0	5.5	1.305	1.229	0.208	0.202	0.466	0.427
6	1000	5.5	1.292	1.186	0.277	0.262	0.492	0.420
7	2000	5.5	1.296	1.181	0.329	0.310	0.526	0.438
8	3000	5.5	1.306	1.182	0.372	0.346	0.556	0.463
9	0	6	1.317	1.216	0.209	0.200	0.465	0.435
10	1000	6	1.320	1.159	0.282	0.258	0.487	0.425
11	2000	6	1.338	1.156	0.347	0.309	0.517	0.447
12	3000	6	1.354	1.170	0.399	0.352	0.543	0.477

In terms of the RWA ratio, Case 3 displays an RWA ratio closer to 1 in comparison to the rest of the 11 cases, where the values are inconsistent. In order to exhibit a more consistent performance, the weighting matrices would require re-tuning for every scenario based on the desired performance, which is not a practical approach as parametric changes are unpredictable and occur frequently.

Figures 6.6 and 6.7 illustrate the lateral acceleration and yaw rate responses of Case 12. Under a rapid SLC maneuver at a constant speed of 100 km/h, the passive vehicle combination displayed distinct oscillations owing to the high payload weight and large CG distance from the hitch. On the application of the LQR-based ATS controller, the peak lateral acceleration of the trailer reduced slightly. However, the controller was unable to significantly reduce the oscillations experienced by the pickup truck-trailer combination. Moreover, throughout the maneuver, both the controlled and uncontrolled vehicle combinations exhibited similar lateral displacements of axle 4 from the desired path, as depicted in Figure 6.8.

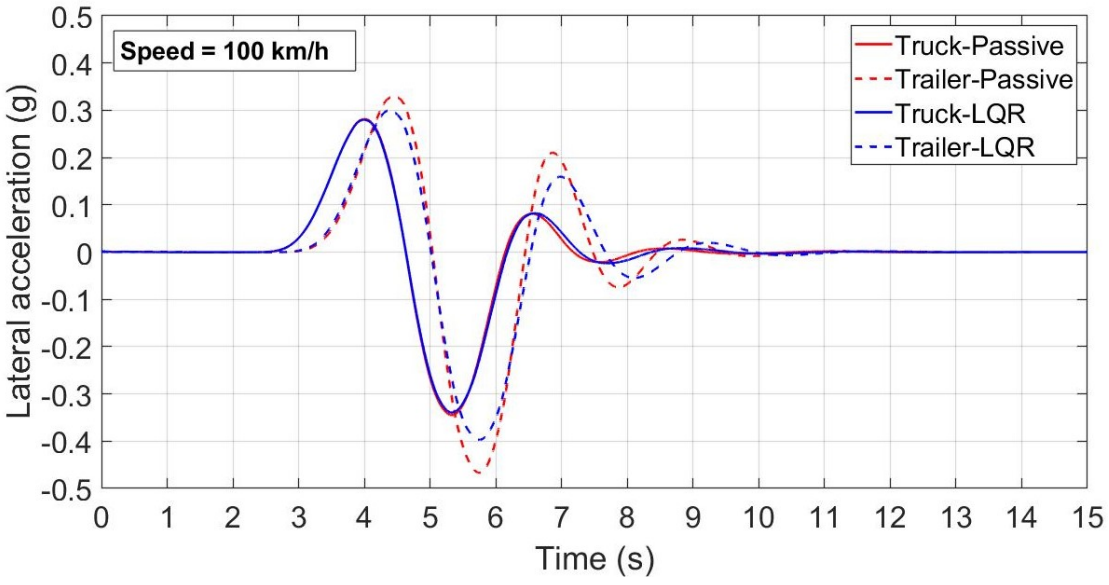

FIGURE 6.6: Lateral acceleration responses for the Case 12 TruckSim model with and without the LQR-based ATS

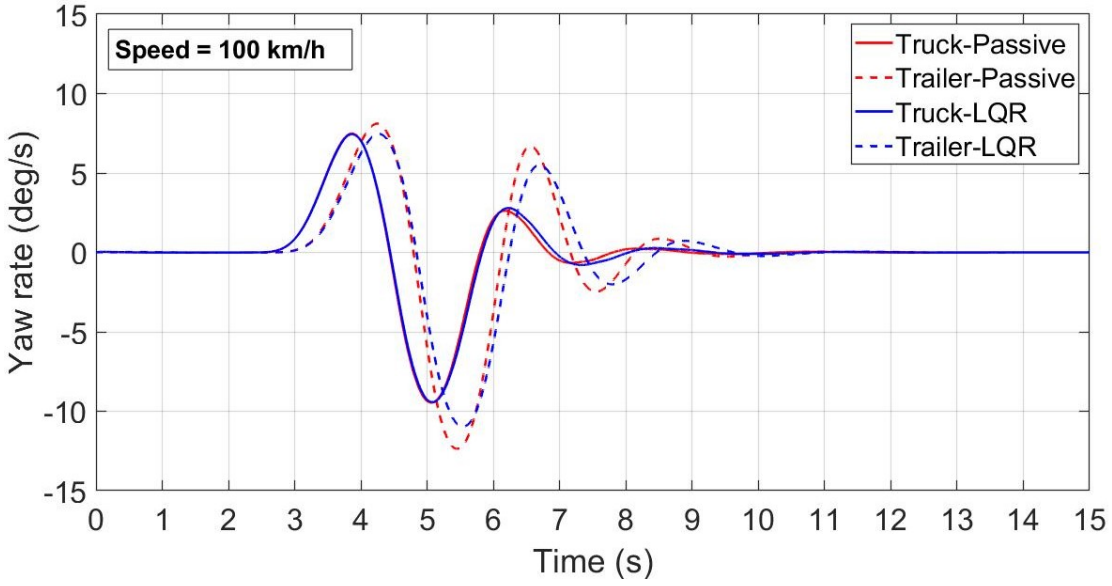

FIGURE 6.7: Yaw rate responses for the Case 12 TruckSim model with and without the LQR-based ATS

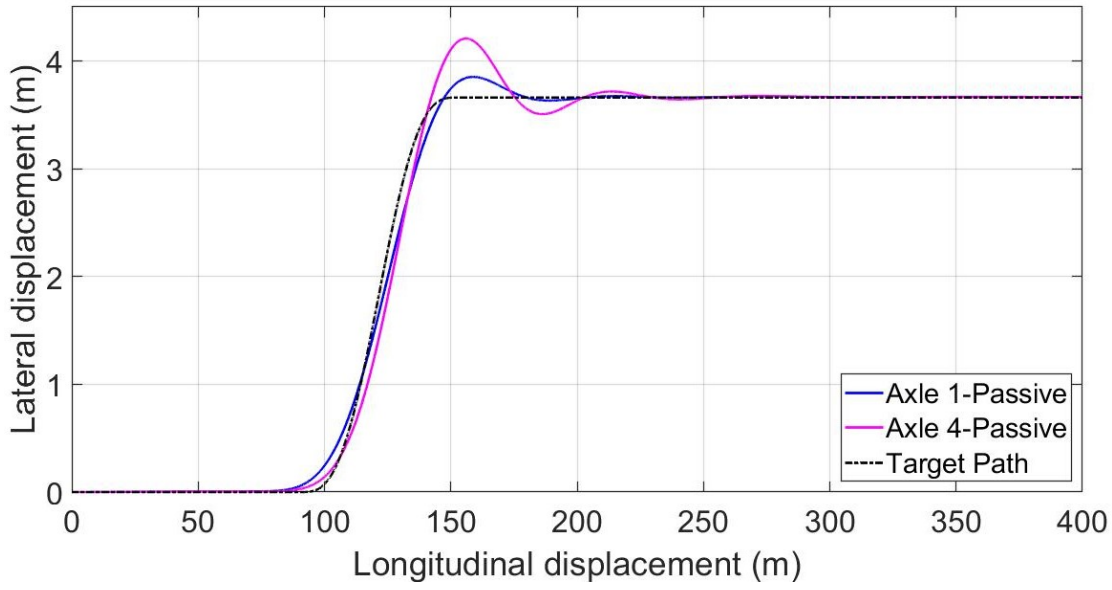

(a)

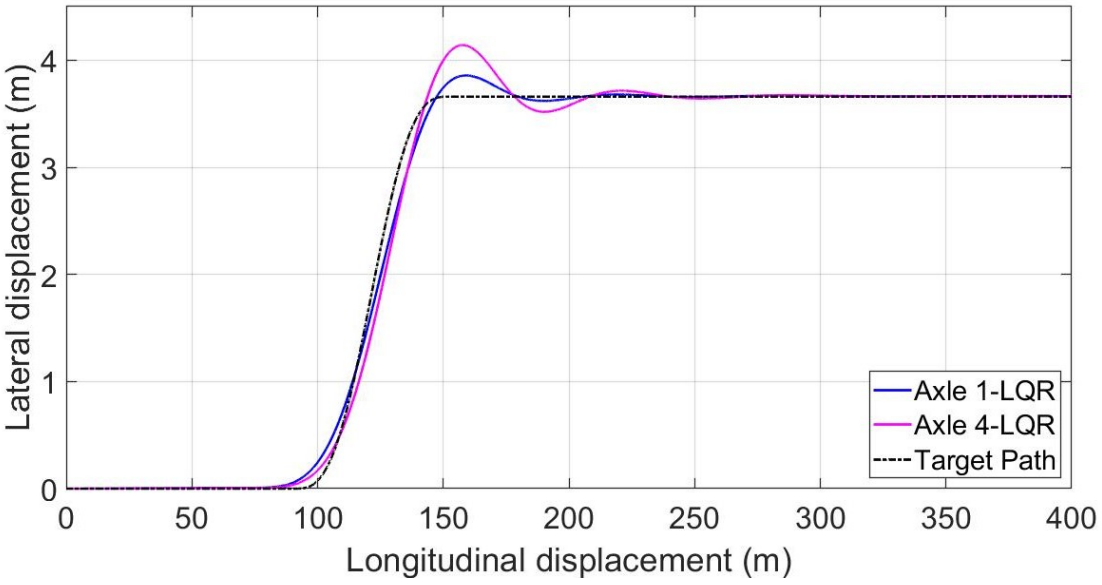

(b)

FIGURE 6.8: Trajectories of axles 1 and 4 for the Case 12 TruckSim model (a) without and (b) with LQR-based ATS

6.3 H_∞-based ATS Controller

The efficiency of the H_∞-based ATS controller was also evaluated under the closed-loop maneuver described in Section 6.1. Similar to the LQR control system, the weighting functions for the H_∞ controller were manually fine-tuned using trial and error method to achieve the desired system performance. Since the LQR-based ATS system demonstrated unsatisfactory results in Section 6.2.2, Case 12 was re-evaluated using the H_∞-based ATS system.

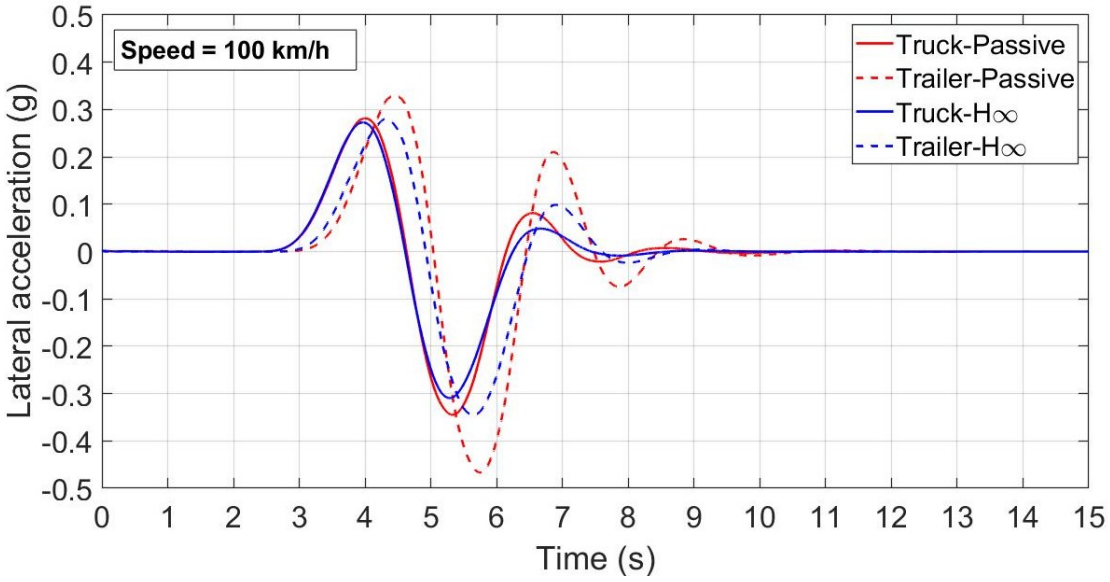

FIGURE 6.9: Lateral acceleration responses for the Case 12 TruckSim model with and without H_∞-based ATS

Figure 6.9 shows the lateral acceleration responses of the TruckSim model with and without the H_∞ controller. Results suggest that the controller augments the performance of the vehicle under the evasive SLC maneuver. In comparison to the LQR controller, the H_∞ controller not only reduced the peak lateral accelerations of both the units but also distinctly reduced overshoot and dampened the oscillations experienced by the vehicle.

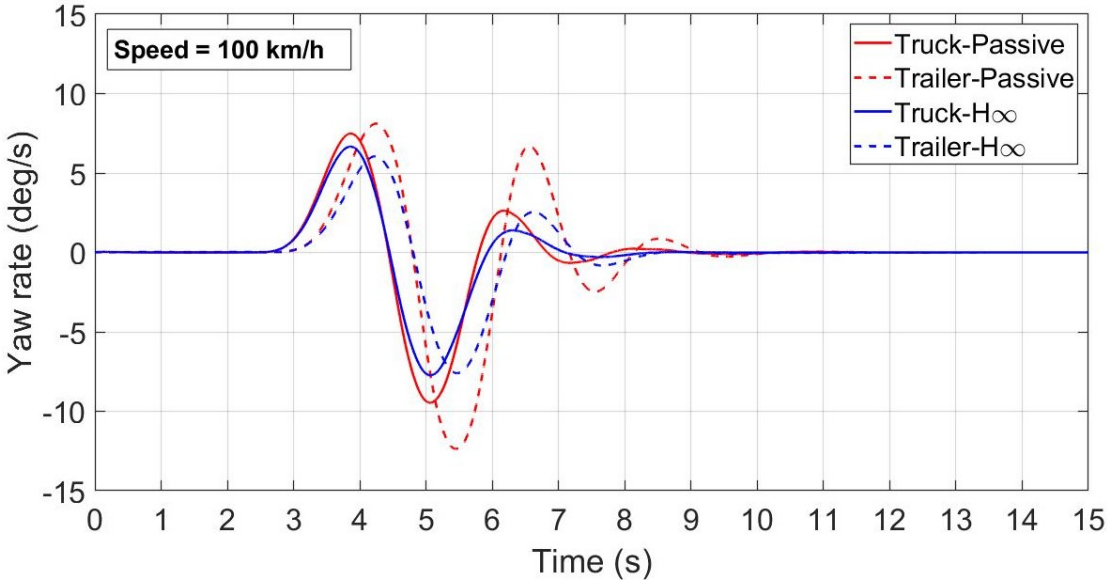

FIGURE 6.10: Yaw rate responses for the Case 12 TruckSim model with and without H_∞-based ATS

Figure 6.10 illustrates the yaw rate responses of the passive and controlled vehicles. It is observed that with the H_∞-based ATS, the system experienced significant reduction in peak yaw rates along with decreased settling time.

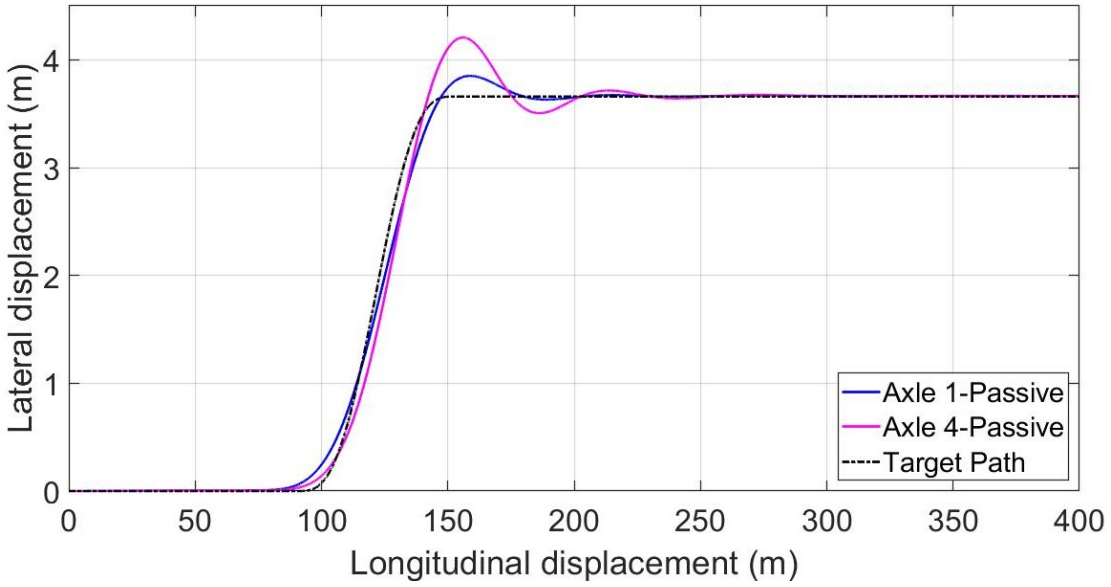

(a)

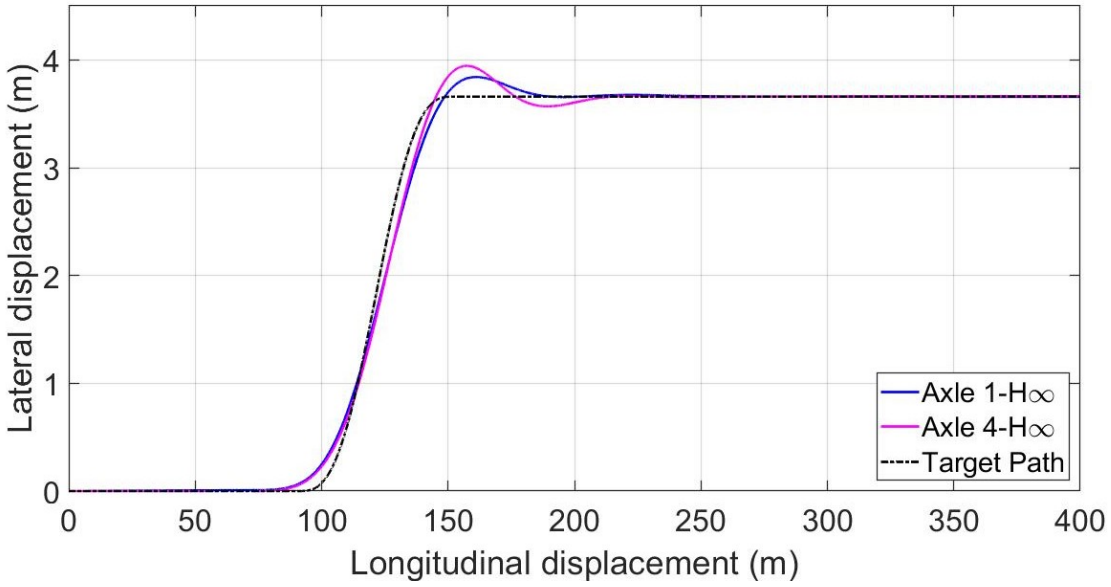

(a) (b)

FIGURE 6.11: Trajectories of axles 1 and 4 for the Case 12 TruckSim model (a) without and (b) with H_∞-based ATS

Figure 6.11 compares the lateral displacement of axles 1 and 4 of the baseline vehicle and the H_∞-based ATS vehicle. Results demonstrate that the H_∞ controlled vehicle experienced reduced lateral deviation of the axles from its intended path. Moreover, the H_∞ controller was also able to closely match the desired trajectory, resulting in better vehicle performance while negotiating a swift SLC maneuver.

TABLE 6.4: Performance evaluation of the TruckSim model with and without the H_∞-based ATS system

Payload weight	**CG distance**	**RWA ratio**		**LTR**		**Offtracking (m)**	
(kg)	**(m)**	Passive	H_∞	Passive	H_∞	Passive	H_∞
3000	6	1.354	1.113	0.399	0.314	0.543	0.287

A summary of the performance measures carried out on the controlled and uncontrolled systems is presented in Table 6.4. The application of H_∞-based

ATS to the vehicle improved the RWA ratio by 17.8%. The LTR demonstrated an improvement of 21.3% and in terms of offtracking, the passive system witnessed an improvement of 47.1% with the H_∞ controller. Furthermore, the values recorded for RWA, LTR and offtracking demonstrated considerable improvement with the H_∞-based ATS controller in comparison to those obtained with the LQR-based controller (Case 12 in Table 6.3).

6.4 Performance comparison of the LQR-based and H_∞-based ATS controllers under varying system parameters

In order to justify the reliability and robustness of the proposed H_∞-based ATS system, the controller was applied to 12 scenarios with varying operating parameters. The scenarios were then evaluated on the basis of the three performance measures previously used and comparison between the LQR-based and H_∞-based ATS controller is carried out. A significant and consistent improvement in the RWA, LTR and offtracking values were observed in all the cases with the robust H_∞-based ATS controller. The results obtained indicate better overall performance of the system with the H_∞-based ATS controller than that with the LQR-based ATS controller. Tables 6.5-6.7 represent the performance of the configurations under passive and active states. Additionally, in the following subsections, an in-depth sensitivity analysis was carried out to interpret the effect of varying parameters on the stability and performance of the vehicle combination.

6.4.1 Varying payload weights and constant CG distances

A comprehensive study on the effect of varying payload weights was carried out to analyze the dynamic stability of the pickup truck-trailer combination. Tables 6.5-6.7 highlight the performance of the various scenarios with and without the implemented LQR-based and H_∞-based controllers.

At a constant payload CG distance of 5 m from the hitch, a slight reduction in RWA values indicates that the stability of the combination was favourable in the presence of a payload. When the payload CG distance was located further away at 5.5 m, an approximately steady RWA is maintained with increasing payload weights. Finally, at a payload CG distance of 6 m from the hitch, a slight increase in the RWA values was noticed. This is indicative of the fact that increase in payload weight at a CG distance farthest away from the hitch leads to instabilities in the vehicle combination. In terms of LTR, an increase in trailer's payload weight resulted in an increase in load transfer between the left and right sides of the vehicle combination. Additionally, increase in trailer's payload weight resulted in an increase in lateral displacement between the last axle and the intended path of the vehicle and therefore, offtracking increased.

TABLE 6.5: RWA measure of the pickup truck-trailer combination with and without the ATS controllers

Case No.	**Weight (kg)**	**CG (m)**	**RWA**		
			Passive	LQR	H_∞
1	0	5	1.315	1.257	1.088
2	1000	5	1.274	1.211	1.055
3	2000	5	1.267	1.081	1.057
4	3000	5	1.269	1.201	1.059
5	0	5.5	1.305	1.229	1.079
6	1000	5.5	1.292	1.186	1.073
7	2000	5.5	1.296	1.181	1.078
8	3000	5.5	1.306	1.182	1.084
9	0	6	1.317	1.216	1.076
10	1000	6	1.320	1.159	1.089
11	2000	6	1.338	1.156	1.101
12	3000	6	1.354	1.170	1.113

TABLE 6.6: LTR measure of the pickup truck-trailer combination with and without the ATS controllers

Case No.	**Weight (kg)**	**CG (m)**	**LTR**		
			Passive	LQR	H_∞
1	0	5	0.277	0.203	0.180
2	1000	5	0.276	0.265	0.234
3	2000	5	0.326	0.265	0.274
4	3000	5	0.365	0.350	0.307
5	0	5.5	0.208	0.202	0.179
6	1000	5.5	0.277	0.262	0.232
7	2000	5.5	0.329	0.310	0.274
8	3000	5.5	0.372	0.346	0.307
9	0	6	0.209	0.200	0.178
10	1000	6	0.282	0.258	0.232
11	2000	6	0.347	0.309	0.277
12	3000	6	0.399	0.352	0.314

TABLE 6.7: Offtracking measure of the pickup truck-trailer combination with and without the ATS controllers

Case No.	Weight (kg)	CG (m)	Offtracking (m)		
			Passive	LQR	H_∞
1	0	5	0.472	0.436	0.278
2	1000	5	0.504	0.440	0.281
3	2000	5	0.543	0.302	0.298
4	3000	5	0.580	0.495	0.317
5	0	5.5	0.466	0.427	0.276
6	1000	5.5	0.492	0.420	0.276
7	2000	5.5	0.526	0.438	0.284
8	3000	5.5	0.556	0.463	0.294
9	0	6	0.465	0.435	0.268
10	1000	6	0.487	0.425	0.272
11	2000	6	0.517	0.447	0.280
12	3000	6	0.543	0.477	0.287

6.4.2 Varying CG distances and constant payload weights

A similar analysis was carried out to investigate the effect of varying payload longitudinal CG distances on the performance of the pickup truck-trailer combination. Tables 6.8-6.10 depict the performance of the vehicle combination at varying payload longitudinal CG distances, with and without the LQR-based and H_∞-based ATS controllers.

In terms of RWA ratio, the overall behaviour of the system indicated that increase in payload CG distances caused the RWA ratio to increase. This implies that the lateral stability of the vehicle tends to reduce with increasing payload longitudinal CG distances, the effect of which is more prominent at higher payload weights. The recorded LTR values did not change drastically with increase in payload CG distances from the hitch. However, the overall behaviour in terms of LTR suggests that increase in CG distances increased the LTR values and the effect again, is more noticeable at higher payload weights. In terms of offtracking, the deviation of the last axle from its intended path increases with increase in the payload's longitudinal CG distances.

TABLE 6.8: RWA measure of the pickup truck-trailer combination with and without the ATS controllers

Case No.	**Weight (kg)**	**CG (m)**	**RWA**		
			Passive	LQR	H_∞
1	0	5	1.315	1.257	1.088
2	0	5.5	1.305	1.229	1.079
3	0	6	1.317	1.216	1.076
4	1000	5	1.274	1.211	1.055
5	1000	5.5	1.292	1.186	1.073
6	1000	6	1.320	1.159	1.089
7	2000	5	1.267	1.081	1.057
8	2000	5.5	1.296	1.181	1.078
9	2000	6	1.338	1.156	1.101
10	3000	5	1.269	1.201	1.059
11	3000	5.5	1.306	1.182	1.084
12	3000	6	1.354	1.170	1.113

TABLE 6.9: LTR measure of the pickup truck-trailer combination with and without the ATS controllers

Case No.	**Weight (kg)**	**CG (m)**	**LTR**		
			Passive	LQR	H_∞
1	0	5	0.277	0.203	0.180
2	0	5.5	0.208	0.202	0.179
3	0	6	0.209	0.200	0.178
4	1000	5	0.276	0.265	0.234
5	1000	5.5	0.277	0.262	0.232
6	1000	6	0.282	0.258	0.232
7	2000	5	0.326	0.265	0.274
8	2000	5.5	0.329	0.310	0.274
9	2000	6	0.347	0.309	0.277
10	3000	5	0.365	0.350	0.307
11	3000	5.5	0.372	0.346	0.307
12	3000	6	0.399	0.352	0.314

TABLE 6.10: Offtracking measure of the pickup truck-trailer combination with and without the ATS controllers

Case No.	**Weight (kg)**	**CG (m)**	**Offtracking (m)**		
			Passive	LQR	H_∞
1	0	5	0.472	0.436	0.278
2	0	5.5	0.466	0.427	0.276
3	0	6	0.465	0.435	0.268
4	1000	5	0.504	0.440	0.281
5	1000	5.5	0.492	0.420	0.276
6	1000	6	0.487	0.425	0.272
7	2000	5	0.543	0.302	0.298
8	2000	5.5	0.526	0.438	0.284
9	2000	6	0.517	0.447	0.280
10	3000	5	0.580	0.495	0.317
11	3000	5.5	0.556	0.463	0.294
12	3000	6	0.543	0.477	0.287

6.5 Summary

This chapter begins with the evaluation of the ATS system using the LQR control technique. The simulations were carried out in TruckSim-MATLAB/Simulink co-simulation environment. The emulated test procedure was a rapid closed-loop SLC maneuver, at a constant forward speed of 100 km/h. The behaviour of the vehicle combination was evaluated on the basis of three performance measures, namely, RWA, LTR and offtracking. From the results obtained, it can

be concluded that the LQR controller was unable to function effectively in the presence of parameter variations.

To address these robustness concerns, the robust H_∞ controller was implemented to design the ATS system. The vehicle combination was subjected to the aforementioned SLC maneuver, under various parametric uncertainties. Results suggest that the robust H_∞ controller effectively augmented the performance of the pickup truck-trailer combination. The H_∞ controller was capable of reducing peak lateral accelerations, yaw rates and also improved the overall dynamic behaviour of the system while negotiating an evasive SLC maneuver.

Chapter 7

Conclusions and Future Work

7.1 Conclusions

The main objective of this study was to improve the stability and maneuverability of a pickup truck-trailer combination at high speeds. As established in previous chapters, articulated vehicles are susceptible to unstable motion modes that can result in fatality. Based on a comprehensive literature review, an active safety technique called Active Trailer Steering (ATS) system was adopted to preserve the performance and behaviour of the pickup truck-trailer combination under rapid, high-speed maneuvers.

The most fundamental step to designing a control system is the derivation of a mathematical representation of the vehicle system to be controlled. To establish the fidelity of the derived linear 3-DOF model, it was validated against a nonlinear TruckSim model under an SLC maneuver at a constant forward speed of 60 km/h. Results indicated reasonable agreement in terms of lateral accelerations and yaw rates of both the pickup truck and trailer. Finally, the stability boundaries of the mathematical model were determined based on an

eigenvalue stability analysis.

The validated yaw-plane linear model was then utilized to design an ATS controller using the Linear Quadratic Regulator (LQR) control technique. Numerical simulations were executed using TruckSim-MATLAB/Simulink co-simulation environment, under a closed-loop SLC maneuver at a constant forward speed of 100 km/h. Results suggest that the combination vehicle with the LQR-based ATS controller outperformed the passive combination vehicle. However, on varying certain trailer parameters, the LQR-based ATS controller did not perform as effectively. This is because the LQR controller was tuned to demonstrate favourable dynamic performance under a specific set of system parameters. This aspect lead to the proposal of a robust $H\infty$-based ATS system.

The $H\infty$-based ATS controller was also developed using the validated 3-DOF linear model, and numerical simulations were carried out similarly, as mentioned above. Results imply that the robust controller can effectively improve the lateral stability and maneuverability of the pickup truck-trailer combination under parametric variations. The $H\infty$-based ATS controller not only reduced the peak lateral accelerations of both the units, but also reduced the overshoot and dampened the oscillations experienced by the vehicle. This indicates that it improved the overall performance of the configuration at high speeds. Moreover, application of safety-related performance measures indicated that the $H\infty$-based ATS system is an assuring solution for the safety enhancement of articulated vehicles. Therefore, it can be concluded that the $H\infty$ controller for the synthesis of ATS systems enhances the performance of the pickup truck-trailer combination, even under a range of parametric uncertainties, and is, therefore, a promising control technique.

7.2 Future Work

- The roll dynamics can be further studied by considering the roll motions of the pickup truck and trailer vehicle units. Once the roll motions are incorporated, the yaw-plane model becomes a yaw-roll linear model with a 5-DOF.

- The results obtained using the $H\infty$ control system can be further authenticated by the implementation of HIL-RT simulations.

- The proposed control system can also be validated in a DHIL vehicle simulator to analyze the behaviour of a human driver on the performance of the controller under various maneuvers.

References

[1] Da-Wei Gu, Petko Petkov, and Mihail M Konstantinov. *Robust control design with MATLAB®*. Springer Science & Business Media, 2013.

[2] Xuejun Ding, Yuping He, Jing Ren, and Tao Sun. A comparative study of control algorithms for active trailer steering systems of articulated heavy vehicles. In *2012 American Control Conference (ACC)*, pages 3617–3622. IEEE, 2012.

[3] Aivis Grislis. Longer combination vehicles and road safety. *Transport*, 25 (3):336–343, 2010.

[4] Tao Sun. Design synthesis of car-trailer systems with active trailer differential braking strategies. Master's thesis, University of Ontario Institute of Technology, Canada, 2013.

[5] Eungkil Lee. Design optimization of active trailer differential braking systems for car-trailer combinations. Master's thesis, University of Ontario Institute of Technology, Canada, 2016.

[6] Xiaodi Kang and Weiwen Deng. Vehicle-trailer handling dynamics and stability control[U+2500] an engineering review. Technical report, SAE Technical Paper, 2007.

[7] U.S. Department of Energy. Vehicle weight classes categories (online). https://afdc.energy.gov/data/.

[8] Featherlite Trailers. Bumper pull trailers vs. gooseneck trailers. https://www.fthr.com/owner-support/trailer-use-and-care/bumper-pull-trailers-vs-gooseneck-trailers.

[9] Ministry of Transportation of Ontario. Ministry of transportation of ontario driver's handbook. https://www.ontario.ca/document/official-mto-drivers-handbook/towing/, April 4, 2017.

[10] Aleksander Hac, Daniel Fulk, and Hsien Chen. Stability and control considerations of vehicle-trailer combination. *SAE International Journal of Passenger Cars-Mechanical Systems*, 1(2008-01-1228):925–937, 2008.

[11] National Highway Traffic Safety Administration. Traffic safety facts 2005 - a compilation of motor vehicle crash data from the fatality analysis reporting system and the general estimates system. `https://www.ontario.ca/document/official-mto-drivers-handbook/towing/`, 2005.

[12] Tushita Sikder. Design of active trailer steering systems for long combination vehicles using robust control techniques. Master's thesis, University of Ontario Institute of Technology, Canada, 2017.

[13] BA Jujnovich and D Cebon. Path-following steering control for articulated vehicles. *Journal of Dynamic Systems, Measurement, and Control*, 135(3): 031006, 2013.

[14] Caizhen Cheng, Richard Roebuck, Andrew Odhams, and David Cebon. High-speed optimal steering of a tractor–semitrailer. *Vehicle system dynamics*, 49(4):561–593, 2011.

[15] Saurabh Kapoor. Fault-tolerant control of active trailer steering systems for multi-trailer articulated heavy vehicles. Master's thesis, University of Ontario Institute of Technology, Canada, 2017.

[16] Laszlo Palkovics and Moustafa El-Gindy. Examination of different control strategies of heavy-vehicle performance. *Journal of dynamic systems, measurement, and control*, 118(3):489–498, 1996.

[17] Deepa S Warrier. Modelling and analysis of active vehicle steering control using nonlinear controller. *International Journal of Advanced Research in Electrical, Electronics and Instrumentation Engineering*, pages 1–11, 2017.

[18] Eungkil Lee, Saurabh Kapoor, Tushita Sikder, and Yuping He. An optimal robust controller for active trailer differential braking systems of car-trailer combinations. *International Journal of Vehicle Systems Modelling and Testing*, 12(1-2):72–93, 2017.

[19] Robert D Ervin. *The influence of weights and dimensions on the stability and control of heavy duty trucks in Canada*. 1986.

[20] P Fancher and C Winkler. Directional performance issues in evaluation and design of articulated heavy vehicles. *Vehicle System Dynamics*, 45(7-8):607–647, 2007.

[21] M Ei-Gindy, N Mrad, and X Tong. Sensitivity of rearward amplication control of a truck/full trailer to tyre cornering stiffness variations. *Proceedings of the Institution of Mechanical Engineers, Part D: Journal of Automobile Engineering*, 215(5):579–588, 2001.

[22] Md Islam et al. Design synthesis of articulated heavy vehicles with active trailer steering systems. Master's thesis, University of Ontario Institute of Technology, Canada, 2010.

[23] JP Thomas and M El-Gindy. Path compliance in lane-change tests designed to evaluate rearward amplification. *Road Transport Technology, University of Michigan Transportation Research Institution, Ann Arbor*, 4:473–482, 1995.

[24] ISO14791. Road vehicles-heavy commercial vehicle combinations and articulated buses-lateral stability test methods. Technical report, Tech. rep, 2002.

[25] Sogol Kharrazi, Mathias Lidberg, and Jonas Fredriksson. A generic controller for improving lateral performance of heavy vehicle combinations. *Proceedings of the Institution of Mechanical Engineers, Part D: Journal of Automobile Engineering*, 227(5):619–642, 2013.

[26] Jo Yung Wong. *Theory of ground vehicles*. John Wiley & Sons, 2008.

[27] Priya Shastry, Moustafa El-Gindy, and Nam Nguyen. Pickup truck and trailer gross vehicle weight study. Technical report, SAE Technical Paper, 2019.

[28] M El-Gindy. An overview of performance measures for heavy commercial vehicles in north america. *International Journal of Vehicle Design*, 16(4-5): 441–463, 1995.

[29] Edward F Kurtz Jr Professor and Ronald J Anderson. Handling characteristics of car-trailer systems; a state-of-the-art survey. *Vehicle System Dynamics*, 6(4):217–243, 1977.

[30] RL Collins and JP Wong. Stability of car trailer systems with special regard to trailer design. *Journal of Dynamic Systems, Measurement, and Control*, 96 (2):236–243, 1974.

[31] Jocelyn Darling, Derek Tilley, and B Gao. An experimental investigation of car—trailer high-speed stability. *Proceedings of the Institution of Mechanical Engineers, Part D: Journal of Automobile Engineering*, 223(4):471–484, 2009.

[32] Ossama Mokhiamar. Stabilization of car-caravan combination using independent steer and drive/or brake forces distribution. *Alexandria Engineering Journal*, 54(3):315–324, 2015.

[33] M. Plöchl, P. Lugner, and A. Riepl. Improvements of passenger car-trailer behaviour by a trailer based control system. *Vehicle System Dynamics*, 29 (sup1):438–450, 1998. doi: 10.1080/00423119808969577.

[34] D Fratila and J Darling. Simulation of coupled car and caravan handling behaviour. *Vehicle System Dynamics*, 26(6):397–429, 1996.

[35] Gašper Šušteršič, Ivan Prebil, and Miha Ambrož. The snaking stability of passenger cars with light cargo trailers. *Strojniški vestnik-Journal of Mechanical Engineering*, 60(9):539–548, 2014.

[36] RS Sharp and MA Alonso Fernandez. Car—caravan snaking: Part 1: The influence of pintle pin friction. *Proceedings of the Institution of Mechanical Engineers, Part C: Journal of Mechanical Engineering Science*, 216(7):707–722, 2002.

[37] RJ Anderson and EF Kurtz Jr. Handling—characteristics simulations of car–trailer systems. *SAE Transactions*, pages 2097–2113, 1980.

[38] Weiwen (Kevin) Deng and Xiaodi Kang. Parametric study on vehicle-trailer dynamics for stability control. *SAE Technical Paper Series*, 2003. doi: 10.4271/2003-01-1321.

[39] T Sun, Y He, E Esmailzadeh, and J Ren. Lateral stability improvement of car-trailer systems using active trailer braking control. *Journal of Mechanics Engineering and Automation*, 2(9):555–562, 2012.

[40] J. R. Ellis. *Vehicle handling dynamics*. Mechanical Engineering Publications, 1994.

[41] Rafay Shamim, Md Manjurul Islam, and Yuping He. A comparative study of active control strategies for improving lateral stability of car-trailer systems. Technical report, SAE Technical Paper, 2011.

[42] Smitha Vempaty and Yuping He. A review of car-trailer lateral stability control approaches. Technical report, SAE Technical Paper, 2017.

[43] Yuping He and Jing Ren. A comparative study of car-trailer dynamics models. *SAE Int. J. Passeng. Cars - Mech. Syst.*, 6:177–186, 04 2013. doi: 10.4271/2013-01-0695. URL https://doi.org/10.4271/2013-01-0695.

[44] Jae Young Kang, George Burkett, Duane Bennett, and Steven A Velinsky. Nonlinear vehicle dynamics and trailer steering control of the towplow, a steerable articulated snowplowing vehicle system. *Journal of Dynamic Systems, Measurement, and Control*, 137(8):081005, 2015.

[45] Md Manjurul Islam, Yuping He, Shenjin Zhu, and Qiushi Wang. A comparative study of multi-trailer articulated heavy-vehicle models. *Proceedings of the Institution of Mechanical Engineers, Part D: Journal of Automobile Engineering*, 229(9):1200–1228, 2015.

[46] Transport Canada. Electronic stability control systems for light vehicles. http://www.tc.gc.ca/media/documents/acts-regulations/TSD-126-E-Rev2.pdf/.

[47] Ken Koibuchi, Masaki Yamamoto, Yoshiki Fukada, and Shoji Inagaki. Vehicle stability control in limit cornering by active brake. Technical report, SAE technical paper, 1996.

[48] Mutaz Keldani and Yuping He. Design of electronic stability control (esc) systems for car-trailer combinations. 2018.

[49] Hensley Mfg. How the hensley hitch works. https://www.hensleymfg.com/faq/hensley-hitch-works/.

[50] Equal i zer. How equal-i-zer works. https://www.equalizerhitch.com/how-equalizer-works/.

[51] Francesco Sorge. On the sway stability improvement of car–caravan systems by articulated connections. *Vehicle System Dynamics*, 53(9):1349–1372, 2015.

[52] H Prem and K Atley. Performance evaluation of the trackaxle (tm) steerable axle system. In *International Symposium on Heavy Vehicle Weights and Dimensions, 7th, 2002, Delft, The Netherlands*, 2002.

[53] Tianjun Zhu, Changfu Zong, Hongyu Zheng, Chengwei Tian, and Hongyan Zheng. Yaw/roll stability modeling and control of heavytractor-semitrailer. Technical report, SAE Technical Paper, 2007.

[54] RC Lin, David Cebon, and DJ Cole. Active roll control of articulated vehicles. *Vehicle System Dynamics*, 26(1):17–43, 1996.

[55] David John Matthew Sampson. *Active roll control of articulated heavy vehicles*. PhD thesis, University of Cambridge Cambridge, UK, 2000.

[56] BP Minaker and J Maiorana. Active control of trailer dynamics using variable geometry. In *Proceedings of the CSME Forum*, pages 1–4, 2004.

[57] Nobuo Hata, Shunichi Hasegawa, Ken Ito, Takeshi Fujishiro, et al. A control method for 4ws truck to suppress excursion of a body rear overhang. Technical report, SAE Technical Paper, 1989.

[58] Ikurou Notsu, Sadahiro Takahashi, and Yoshito Watanabe. Investigation into turning behavior of semi-trailer with additional trailer-wheel steering–a control method for trailer-wheel steering to minimize trailer rear-overhang swing in short turns. Technical report, SAE Technical Paper, 1991.

[59] AMC Odhams, RL Roebuck, BA Jujnovich, and D Cebon. Active steering of a tractor–semi-trailer. *Proceedings of the Institution of Mechanical Engineers, Part D: Journal of Automobile Engineering*, 225(7):847–869, 2011.

[60] Caizhen Cheng and David Cebon. Improving roll stability of articulated heavy vehicles using active semi-trailer steering. *Vehicle System Dynamics*, 46(S1):373–388, 2008.

[61] K Rangavajhula and HS J Tsao. Command steering of trailers and command-steering-based optimal control of an articulated system for tractor-track following. *Proceedings of the Institution of Mechanical Engineers, Part D: Journal of Automobile Engineering*, 222(6):935–954, 2008.

[62] M Abroshan, M Taiebat, A Goodarzi, and A Khajepour. Automatic steering control in tractor semi-trailer vehicles for low-speed maneuverability enhancement. *Proceedings of the Institution of Mechanical Engineers, Part K: Journal of Multi-body Dynamics*, 231(1):83–102, 2017.

[63] A Dolly Mary, Abraham T Mathew, and Jeevamma Jacob. A robust h-infinity control approach of uncertain tractor trailer system. *IETE Journal of Research*, 59(1):38–47, 2013.

[64] Maliheh Sadeghi Kati, Hakan Köroğlu, and Jonas Fredriksson. Robust lateral control of long-combination vehicles under moments of inertia and tyre cornering stiffness uncertainties. *Vehicle System Dynamics*, pages 1–27, 2018.

[65] Taehyun Shim, Sehyun Chang, and Seok Lee. Investigation of sliding-surface design on the performance of sliding mode controller in antilock braking systems. *IEEE Transactions on Vehicular Technology*, 57(2):747–759, 2008.

[66] Mohammad Amin Saeedi, Reza Kazemi, and Shahram Azadi. Improvement in the rollover stability of a liquid-carrying articulated vehicle via a new robust controller. *Proceedings of the Institution of Mechanical Engineers, Part D: Journal of Automobile Engineering*, 231(3):322–346, 2017.

[67] Shenjin Zhu, Yuping He, and Jing Ren. On robust controllers for active steering systems of articulated heavy vehicles. *International Journal of Heavy Vehicle Systems*, 26(1):1–30, 2019.

[68] Yuping He and Md Manjurul Islam. An automated design method for active trailer steering systems of articulated heavy vehicles. *Journal of Mechanical Design*, 134(4):041002, 2012.

[69] Yuping He, Md Manjurul Islam, and Timothy D Webster. An integrated design method for articulated heavy vehicles with active trailer steering systems. *SAE International Journal of Passenger Cars-Mechanical Systems*, 3 (2010-01-0092):158–174, 2010.

[70] Kyong-il Kim, Hsin Guan, Bo Wang, Rui Guo, and Fan Liang. Active steering control strategy for articulated vehicles. *Frontiers of Information Technology & Electronic Engineering*, 17(6):576–586, 2016.

[71] Qiushi Wang. Design and validation of active trailer steering systems for articulated heavy vehicles using driver-hardware-in-the-loop real-time simulation. Master's thesis, University of Ontario Institute of Technology, Canada, 2015.

[72] Adam Piłat and Piotr Włodarczyk. The μ-synthesis and analysis of the robust controller for the active magnetic levitation system. *Automatyka/Akademia Górniczo-Hutnicza im. Stanisława Staszica w Krakowie*, 15(1):85–98, 2011.

[73] Mutaz Keldani, Khizar Qureshi, Yuping He, and Ramiro Liscano. Design and optimization of a robust active trailer steering system for car-trailer combinations. Technical report, SAE Technical Paper, 2019.

[74] Zhituo Ni and Yuping He. Design and validation of a robust active trailer steering system for multi-trailer articulated heavy vehicles. *Vehicle System Dynamics*, pages 1–27, 2018.

[75] Matteo Corno, Mara Tanelli, Ivo Boniolo, and Sergio M Savaresi. Advanced yaw control of four-wheeled vehicles via rear active differential braking. In *Proceedings of the 48h IEEE Conference on Decision and Control (CDC) held jointly with 2009 28th Chinese Control Conference*, pages 5176–5181. IEEE, 2009.

[76] Guo-Dong Yin, Nan Chen, Jin-Xiang Wang, and Ling-Yao Wu. A study on μ-synthesis control for four-wheel steering system to enhance vehicle lateral stability. *Journal of dynamic systems, measurement, and control*, 133 (1):011002, 2011.

[77] K David Young, Vadim I Utkin, and Umit Ozguner. A control engineer's guide to sliding mode control. In *Proceedings. 1996 IEEE International Workshop on Variable Structure Systems.-VSS'96-*, pages 1–14. IEEE, 1996.

[78] Arie Levant. Principles of 2-sliding mode design. *automatica*, 43(4):576–586, 2007.

[79] RH Byrne and CT Abdallah. Design of a model reference adaptive controller for vehicle road following. *Mathematical and computer modelling*, 22 (4-7):343–354, 1995.

[80] HM Lv, Nan Chen, and Pu Li. Multi-objective h∞ optimal control for four-wheel steering vehicle based on yaw rate tracking. *Proceedings of the Institution of Mechanical Engineers, Part D: Journal of Automobile Engineering*, 218(10):1117–1123, 2004.

[81] Wan-zhong Zhao, Yi-jun Li, Chun-yan Wang, Ting Zhao, and Xiao-yue Gu. H∞ control of novel active steering integrated with electric power steering function. *Journal of Central South University*, 20(8):2151–2157, 2013.

[82] Huiying Sun and Long Yan. Robust fuzzy control for nonlinear discrete-time stochastic systems with markovian jump and parametric uncertainties. *Mathematical Problems in Engineering*, 2014, 2014.

[83] Bilin Aksun Guvenc, Tilman Bunte, Dirk Odenthal, and Levent Guvenc. Robust two degree-of-freedom vehicle steering controller design. *IEEE Transactions on Control Systems Technology*, 12(4):627–636, 2004.

[84] Bilin Aksun Guvenc, Levent Guvenc, and Sertaç Karaman. Robust yaw stability controller design and hardware-in-the-loop testing for a road vehicle. *IEEE Transactions on Vehicular Technology*, 58(2):555–571, 2009.

[85] Shinichiro Horiuchi, Naohiro Yuhara, and Akihiko Takei. Two degree of freedom/h∞ controller synthesis for active four wheel steering vehicles. *Vehicle System Dynamics*, 25(S1):275–292, 1996.

[86] Pushkar Hingwe, Han-Shue Tan, Andrew K Packard, and Masayoshi Tomizuka. Linear parameter varying controller for automated lane guidance: experimental study on tractor-trailers. *IEEE Transactions on control systems technology*, 10(6):793–806, 2002.

[87] Peter F Sweatman and Scott McFarlane. *Investigation into the specification of heavy trucks and consequent effects on truck dynamics and drivers*. Department of Transport and Regional Services, 2000.

[88] M El-Gindy and JY Wong. A comparison of various computer simulation models for predicting the directional responses of articulated vehicles. *Vehicle System Dynamics*, 16(5-6):249–268, 1987.

[89] Ning Zhang. *Stability Investigation of Car-trailer Combinations based on Time-Frequency Analysis*. PhD thesis, Technische Universität, 2015.

[90] Md Islam et al. *Parallel design optimization of multi-trailer articulated heavy vehicles with active safety systems*. PhD thesis, University of Ontario Institute of Technology, Canada, 2013.

[91] Peter D'Urso. Development of h∞ control strategy for a multi-wheeled combat vehicle. Master's thesis, University of Ontario Institute of Technology, Canada, 2016.

[92] Kemin Zhou and John Comstock Doyle. *Essentials of robust control*, volume 104. Prentice hall Upper Saddle River, NJ, 1998.

[93] Rajesh Rajamani. *Vehicle dynamics and control*. Springer Science & Business Media, 2011.

[94] Shenjin Zhu and Yuping He. A driver-adaptive stability control strategy for sport utility vehicles. *Vehicle system dynamics*, 55(8):1206–1240, 2017.

[95] Jesse Brown. High-speed lateral stability analysis of articulated heavy vehicles using driver-in-the-loop real time simulation. Master's thesis, University of Ontario Institute of Technology, Canada, 2018.

Appendix A

Parameters	Description	Value	Units
m_1	Total mass of pickup truck	2,155.64	kg
I_{z1}	Yaw moment of inertia of the pickup truck	4,103.7	kgm^{2}
r_1	Yaw rate of the pickup truck	N/A	deg/s
V_{y1}	Lateral speed of the pickup truck	N/A	m/s
F_{y1}	Lateral force of the pickup truck's 1^{st} axle	N/A	N
F_{y2}	Lateral force of the pickup truck's 2^{nd} axle	N/A	N
m_2	Total mass of trailer	2,380 / 3,380 / 4,380 / 5,380	kg
I_{z2}	Yaw moment of inertia of the trailer	11,022.0 / 12,688.67 / 14,355.33 / 16,022.0	kgm^{2}
r_2	Yaw rate of the trailer	N/A	deg/s
V_{y2}	Lateral speed of the trailer	N/A	m/s
F_{y3}	Lateral force of the trailer's 1st axle	N/A	N
F_{y4}	Lateral force of the trailer's 2nd axle	N/A	N
U	Forward speed of pickup truck-trailer combination	N/A	m/s
a	Distance between the front axle and the CG of the pickup truck	1.4	m
$b = d$	Distance between the CG and the rear axle of the pickup truck	2.6	m
e	Distance between the hitch and the CG of the trailer	5.5	m
f	Distance between the CG and the first axle of the trailer	0.4	m
g	Distance between the CG and the second axle of the trailer	1.16	m

The system matrices, A and B, of the 3-DOF model where A = $M^{-1}N$ and B = $M^{-1}P$ are described below:

$$\mathrm{M} = \begin{bmatrix} dm_1 & I_{z1} & 0 & 0 \\ m_1 & 0 & m_2 & 0 \\ 0 & 0 & -em_2 & I_{z2} \\ 1 & -d & -1 & -e \end{bmatrix} \qquad \mathrm{N} = \frac{1}{U}\begin{bmatrix} N_{11} & N_{12} & N_{13} & N_{14} \\ N_{21} & N_{22} & N_{23} & N_{24} \\ N_{31} & N_{32} & N_{33} & N_{34} \\ N_{41} & N_{42} & N_{43} & N_{44} \end{bmatrix}$$

$$\mathrm{P} = \begin{bmatrix} -C_1(a+d) & 0 & 0 \\ -C_1 & -C_3 & -C_4 \\ 0 & C_3(e+f) & C_4(e+g) \\ 0 & 0 & 0 \end{bmatrix} \qquad \mathrm{C} = \begin{bmatrix} 1 & 0 & 0 & 0 \\ 0 & 1 & 0 & 0 \\ 0 & 0 & 1 & 0 \\ 0 & 0 & 0 & 1 \end{bmatrix} \qquad \mathrm{D} = \begin{bmatrix} 0 \\ 0 \\ 0 \\ 0 \end{bmatrix}$$

where,

$N_{11} = C_1(a+d) + C_2(d-b)$
$N_{12} = aC_1(a+d) - bC_2(d-b) - dm_1U^2$
$N_{13} = 0$
$N_{14} = 0$

$N_{21} = C_1 + C_2$
$N_{22} = (aC_1 - bC_2) - (m_1U^2)$
$N_{23} = C_3 + C_4$
$N_{24} = (-fC_3 - gC_4) - (m_2U^2)$

$N_{31} = 0$
$N_{32} = 0$
$N_{33} = -C_3(e+f) - C_4(e+g)$
$N_{34} = (fC_3)(e+f) + (gC_4)(e+g) + (em_2U^2)$

$N_{41} = 0$
$N_{42} = -U^2$
$N_{43} = 0$

$N_{44} = U^2$

$$Q = \begin{bmatrix} 0.02 & 0 & 0 & 0 \\ 0 & 0.02 & 0 & 0 \\ 0 & 0 & 0.02 & 0 \\ 0 & 0 & 0 & 0.02 \end{bmatrix}$$

$$R = \begin{bmatrix} 1 & 0 \\ 0 & 1 \end{bmatrix}$$